Robust Stability Analysis and Systematic Design of Single Input Interval Type-2 Fuzzy Logic Controllers

Tufan Kumbasar, *Member, IEEE*

***Abstract*—Recent results on fuzzy control have shown that Interval Type-2 (IT2) Fuzzy Logic Controllers (FLCs) might achieve better control performance due to the additional degree of freedom provided by the Footprint of Uncertainty (FOU) in their IT2 Fuzzy Sets (FSs). However, the design and robust stability analysis of the IT2-FLCs are still challenging problems due to their relatively more complex internal structure. In this paper, we will derive the explicitly FM of a Single input IT2-FLC (SIT2-FLC) to present design methods and investigate its robustness. The analytical information of the IT2-FM will give the opportunity to provide explanations on the roles of the FOU parameters by taking advantage of the well-developed framework of nonlinear control theory. Comparative theoretical explorations will be presented on the differences between the Type-1 (T1) FM and IT2-FM to clearly show the role of the FOU on the robust control system performance. It will be proven that the robust stability of the IT2 fuzzy system is guaranteed with the aids of the well-known Popov-Lyapunov method. Moreover, analytical design methods are presented for SIT2-FLCs to generate commonly employed control curves by only tuning the size of the FOUs without a need of an optimization procedure. It will be theoretically shown that the FOU gives the opportunity to the SIT2-FLC to generate commonly employed nonlinear control curves while also providing a certain degree of robustness which cannot be accomplished by its T1 counterpart. The presented results provide theoretical explanations on the role of the FOU on the performance and robustness of the SIT2-FLC.**

***Index Terms*— Controller Design, Interval Type-2 Fuzzy Logic Controllers, Robustness Analysis**

I. Introduction

Type-1 (T1) Fuzzy Logic Controllers (FLCs) have been widely used as alternatives to conventional controllers [1-10]. It has been stated in [11] that T1-FLCs can be designed using single, two or three inputs. Although the majority of the research work on T1-FLCs focuses on the two-input structures [1-10], it has been shown in various works that Single input T1-FLC (ST1-FLCs) provide greater flexibility and better functional properties [11-17]. Recently, the main research focus is on Interval Type-2 (IT2) FLCs. Generally, IT2-FLCs achieve better performances because of the additional degree of freedom provided by the Footprint of Uncertainty (FOU) in their IT2 Fuzzy Sets (FSs) [18-24]. The internal structure of the IT2-FLC is similar to its T1 counterpart. The major difference is that there is an extra Type Reduction (TR) procedure since IT2-FLCs employ and process IT2-FSs [25-28]. Several studies have been presented to analyze the effect of the FOU and extra TR process on the type-2 Fuzzy Mapping (FM) [28-32]. Yet, usually evolutionary algorithms have been employed to design IT2-FLCs such that to generate a desired FM (i.e. control surface) [18-24]. The main drawback of this approach is the lack of understanding of how the FOU parameters affect the performance and robustness of the IT2-FLC [33-35]. Thus, deriving the analytical structure of an IT2-FLC might be an efficient way to examine the IT2-FLC in the framework of the nonlinear control theory [33-38]. In this context, Wu [28] examined the IT2-FLCs around the steady state and showed that IT2-FLCs are potentially more robust since they provide smoother control surfaces in comparison with their T1 counterparts. Du and Ying [33] also derived analytical expressions for IT2-FLC and represented them as a collection of nonlinear PI/PD controllers with variable gains. Recently, stability tests and control design methods for IT2 Takagi–Sugeno–Kang (TSK) fuzzy systems have been also proposed [36-42]. Yet, the systematic design and robustness analysis of the IT2-FLC are still challenging problems due to its relatively more complex structure [32-43].

In this paper, we will present design methods for Single input IT2-FLCs (SIT2-FLCs) and investigate their robustness based on analytical derivations. The most important feature of the SIT2-FLC is the closed form presentation of its FM. This analytical structure information will give the opportunity to examine the robustness of the SIT2-FLC in the well-developed nonlinear control theory. Moreover, since the IT2-FM is defined in a two dimensional domain, the design problem of the IT2-FLC will be transformed from control surface generation to Control Curve (CC) generation. Thus, in comparison to a T1 fuzzy CC (CC_{T1}), the IT2-FM will be examined to identify the effect of the FOU on the IT2 fuzzy CC (CC_{IT2}) generation. Based on the explicit IT2-FM information, design methods will be presented where precise information about how to tune the FOU size is provided. The benefits of this paper are 1) taking advantage of the nonlinear

This research is supported by the project (113E206) of Scientific and Technological Research Council of Turkey (TUBITAK). All of these supports are appreciated.

T. Kumbasar is with the Control and Automation Engineering Department, Faculty of Electrical and Electronics Engineering, Istanbul Technical University, Istanbul, TR-34469, Turkey (e-mail: kumbasart@itu.edu.tr).

control theory to examine the robustness of SIT2-FLCs 2) providing theoretical explanations on the roles of the FOU parameters on the performance and robustness of the SIT2-FLCs, 3) presenting analytical design methods for SIT2-FLCs without a need of an optimization procedure, 4) providing explanations that a SIT2-FLC might not be implemented by ST1-FLCs which are constructed with more rules and/or various types of Membership Functions (MFs).

In this study, we will start presenting the general structure of the Single Input FLCs (SFLCs) and show that the fuzzy systems can be transformed into the perturbed Lur'e system. It will be then shown that their robust stability is guaranteed if and only if the T1-FM and IT2-FM are symmetrical, continuous and sector bounded mappings. In this context, the FMs will be derived to prove that both handled T1-FM and IT2-FM satisfy the necessary robust stability conditions. Moreover, by analyzing the characteristics of the FMs, theoretical explanations will be provided how their design parameters affect the generated Control Actions (CAs) of the SFLCs. In this context, comparative explorations will be presented on the fundamental differences between the IT2 fuzzy CAs (CA_{IT2}s) and T1 fuzzy CAs (CA_{T1}s). The relative merits of tuning the size of the FOU will be explicitly shown and then design strategies will be presented for SIT2-FLCs composed of 3 and 5 rules. It will be shown that, by tuning the size of the FOU, smooth, aggressive and S-shaped CCs can be generated which cannot be accomplished by its T1 counterpart that is composed of 3 and 5 rules. Comprehensive simulation studies will be provided to illustrate the presented analyses and derivations. It will be also tried to establish if the IT2-FM can be duplicated with various ST1-FLCs since it has been mentioned that an IT2-FS embeds a huge number of T1-FSs [26]. Thus, it will be firstly investigated whether various types of ST1-FLCs (constructed with more rules and/or alternative MFs) can generate the identical CC_{IT2} which is constructed from only 3 rules. It will be shown that the FOU gives the opportunity to generate CC_{IT2}s which cannot be duplicated by its T1 counterparts even though they have more design parameters. Then, results will be presented where the robustness of the SFLCs are examined and compared. It will be firstly illustrated that the stability of two SIT2-FLCs, that have different sizes of FOU, is guaranteed but in different robustness measures. Thus, it will be clearly shown that the size of FOU directly affects the robustness of the SIT2-FLC from a mathematical point of view. It will be also shown that the ST1-FLCs, that were constructed such that to duplicate the CC_{IT2}s, provide different robustness measures and control performances. It will be concluded that the tuning the size of the FOU gives the opportunity to generate CCs such as smooth, aggressive and S-shaped while also providing a certain degree of robustness to system which cannot be provided by ST1-FLC although it has more design parameters.

Section II will present the SFLC system. Section III will present the internal structure of SFLCs and the properties of the FMs. Section IV will present the design methods for SFLCs. Section V will present the simulation results and Section VI will present the conclusions and future work.

II. The Single Input Fuzzy Logic Control System

In this section, the components of the single input fuzzy logic system are presented. It will be shown that the fuzzy control system can be transformed to the perturbed Lur'e system to examine its robust stability under certain conditions.

A. The Components of the SFLCs

The SFLC is constructed by choosing the input as the error signal (e) and the output as the control signal (u). As shown in Fig.1a, the SFLC is cascaded to a baseline PID controller [11]. Thus, if the FM ($\varphi_o(\sigma)$) is a Unit Mapping (UM) as:

$$\varphi_{o_{UM}}(\sigma) = \sigma \tag{1}$$

then the SFLC will reduce to a conventional PID structure.

In the SFLC given in Fig.1a, K_e and K_u are the Scaling Factors (SFs). The input SF K_e is defined such that the input is normalized to the universe of discourse where the antecedent MFs of the SFLC are defined [-1, 1]. Thus, K_e is defined as $K_e=1/(r(t_f)-y(t_f))$ where $r(t_f)$ and $y(t_f)$ are the values at the instant of the reference change $t=t_f$ [11], [43]. Hence, the e value is converted into a σ value which is the actual input of the FM. The output of the SFLC is defined as follows:

$$u = K_u\left(K_P\varphi_o + K_D\frac{d\varphi_o}{dt} + K_I\int_0^t \varphi_o d\xi\right) \tag{2}$$

where φ_o is the output of the (T1 or IT2) FM, K_u is the output SF that is defined as $K_u = {K_e}^{-1}$, K_P, K_D and K_I are the proportional, derivative and integral control gains of the baseline PID controller, respectively. Thus; the controller gain, derivative and integral time constant of the controller are $K_c = K_P$, $\tau_D = K_I/K_P$ and $\tau_I = K_I/K_P$, respectively. It can be seen that the output of the (T1 and IT2) SFLC is analogous to a conventional PID ones [11], [43]. In applications, the differentiator $(d(.)/dt)$ in (2) can be implemented as follows:

$$\frac{d\varphi_o}{dt} \approx \hat{\dot{\varphi}}_o \equiv \frac{s}{1+\epsilon\tau_D s}, \epsilon \le 0.1 \tag{3}$$

where s is the Laplace operator. Now, (2) can be redefined as:

$$\begin{aligned} \dot{x}_c &= A_c x_c + b_c\varphi_o \\ u &= c_c x_c + d_c\varphi_o \end{aligned} \tag{4}$$

where $x_c = [\epsilon\tau_D\hat{\dot{\varphi}}_o - \varphi_o, \int_0^t \varphi_o d\xi]^T \in R^2$ is the state vector of the controller and

$$A_c = \begin{bmatrix} -1/(\epsilon\tau_D) & 0 \\ 0 & 0 \end{bmatrix} \quad b_c = \begin{bmatrix} -1/(\epsilon\tau_D) \\ 1 \end{bmatrix}$$
$$c_c = [K_cK_u/\epsilon \quad K_cK_u/\tau_I] \quad d_c = K_cK_u(1+\epsilon)/\epsilon \tag{1}$$

The design of the SFLC is accomplished in two main steps. At first, the baseline PID is designed by using conventional design methods. Then, the FM is designed such that to enhance the performance while providing a certain degree of robustness to the SFLC [11], [43].

B. Robust Stability of the Fuzzy Logic Control System

A single input single output nonlinear system can be defined as follows:

$$\dot{X}_s = f(X_s, U) \quad Y = c_0^T X_s \tag{7}$$

where $X_s \in R^q$ is the state vector, n is the number of the states, U is the system input and $f \in R^q$ represents the nonlinear mapping. Let $X_s = x_s + x_{s0}$ and $U = u + u_0$ where (x_{s0}, u_0) denotes a nominal operating point. Then, by

expanding the nonlinear system into a Taylor series, we obtain

$$\dot{x}_s = x_s \frac{\partial f}{\partial X_s}\Big|_{(x_{s0},u_0)} + u\frac{\partial f}{\partial U}\Big|_{(x_{s0},u_0)} + g(x_s,u) \quad (7)$$

where $g(x_s,u)$ inherits higher-order terms in x_s, u and the uncertainties of the system. Let A_0 and b_0 denote the Jacobian matrix of $\partial f/\partial X_s$ and $\partial f/\partial U$, then we can define

$$\begin{aligned} \dot{x}_s &= A_{s0}x_s + b_{s0}u + g(x_s,u) \\ y &= c_{s0}x_s \end{aligned} \quad (8)$$

where $c_{s0} = [1 \quad 0 \ldots \quad 0]$. We will be assume that the nominal open-loop transfer function of the system has a relative degree 2 or more, i.e. $c_{s0}b_{s0} = 0$, and the system satisfies $c_{s0}g(x_s,u) = 0$.

In order to examine the stability of the fuzzy system, let $r = 0$. Thus, it can be defined:

$$e = -y = -c_{s0}x_s \quad (9)$$

$$\sigma = K_e e = -K_e c_{s0} x_s \quad (10)$$

Now, let us define a state space model where the output is σ and the input is φ_o. Thus, the control law given in (4) is folded into the system given in (8). Then, we can obtain

$$\begin{aligned} \dot{x} &= A_1 x + b_1\varphi_o + g(x,u) \\ \sigma &= c_1 x \end{aligned} \quad (11)$$

where x is the new state vector defined as $x = [x_c \; x_s]^T$ and A_1, b_1 and c_1 are defined as:

$$A_1 = \begin{bmatrix} A_c & 0 \\ b_{s0}c_c & A_{s0} \end{bmatrix} \quad b_1 = \begin{bmatrix} b_c \\ b_{s0}d_c \end{bmatrix} \quad c_1 = [0 \quad -K_e c_{s0}] \quad (12)$$

The block diagram of the equivalent model is given in Fig.1b. Now, assume that the output of the SFLC is sector bounded $[K_{min}, K_{max}]$. Thus, a normalized FM can be defined as:

$$\varphi(\sigma) = \varphi_o(\sigma) - K_{min}\sigma \quad (13)$$

Then, it can be defined:

$$0 \le \varphi\sigma \le \bar{K}\sigma^2 \text{ for } \forall\sigma \ne 0 \quad (14)$$

where $\bar{K}$ is the normalized upper bound defined as:

$$\bar{K} = K_{max} - K_{min} \quad (15)$$

Thus, the new sector bound will be $[0, \bar{K}]$. Then, an equivalent system can be defined as follows:

$$\begin{aligned} \dot{x} &= Ax - b\varphi(\sigma) + g(x_s,u) \\ \sigma &= c\,x \end{aligned} \quad (16)$$

where

$$A = A_1 - K_{min}b_1c_1 \quad b = -b_1 \quad c = -c_1 \quad (17)$$

The transfer function of this system can then be obtained via:

$$G(s) = c(sI - A)^{-1}b \quad (18)$$

The new block diagram of the system is shown in Fig.1c which is a perturbed Lur'e system [44]. The transformation from Fig.1a to Fig.1c is possible if and only if the FM is a continuous, symmetrical and sector bounded mapping [44], [45]. The robust stability of this SFLC system can be guaranteed via the well-known Popov-Lyapunov method.

Theorem-1: If the system described by (16) satisfies the following conditions, then the equilibrium point $x = 0$ is uniformly asymptotically stable.

C1) The nonlinearity φ always belongs to the sector $[0, \bar{K}]$ where $\bar{K}$ is a positive number**.**

C2) The system matrix A is Hurwitz ($G(s)$ is stable) and there exists a scalar $r > 0$ such that $-1/r \ne \lambda_i$ where λ_i is an eigenvalue of A and

$$1/\bar{K} + Re[(1 + jwr)G(jw)] > 0 \; \forall w \in R \quad (19)$$

C3) Let

$$v = 1/2\,(rA^Tc + c) \quad \gamma = rc^Tb + 1/\bar{K} \quad (20)$$

where r is chosen such that $\gamma \ge 0$. Given a symmetric positive define matrix W; there exists a $\varepsilon > 0$, a vector q, symmetric positive define matrix P and W_0, and $\delta > 0$ satisfiying:

$$\begin{aligned} A^TP + PA &= -qq^T - \varepsilon W \quad Pb - v = \sqrt{\gamma}q \\ \varepsilon W &= \varepsilon W_0 + \delta I \end{aligned} \quad (21)$$

C4) The nonlinearity $g(x,u)$ is bounded and satisfies:

$$\|g(x,u)\|_2 \le \beta\|x\|_2 \le \frac{\delta}{2\|P\|_{i2} + r\bar{K}\|c\|_2^2}\|x\|_2 \quad (22)$$

where β is a robustness measure, $\|P\|_{i2}$ denotes the spectral norm of the matrix P, $\|.\|_2$ represents 2-norm, and M is the domain where $g(x,u)$ is bounded.

Proof: The proof of **C1** will be presented in Section III for the SFLCs. **C2** can be proven via the Popov criterion [45]. **C3** and **C4** can be proven via the Lyapunov function [44], [45]:

$$V(x) = x^TPx + r\int_0^\sigma \varphi(y)dy \quad (23)$$

The stability domain (Ω) where $x = 0$ is stable is then defined as:

$$\Omega = \{x \in R^n | V(x) \le \theta\} \quad (24)$$

Note that the stability domain can be explicitly presented if the FMs can be presented in a closed form presentation. ■

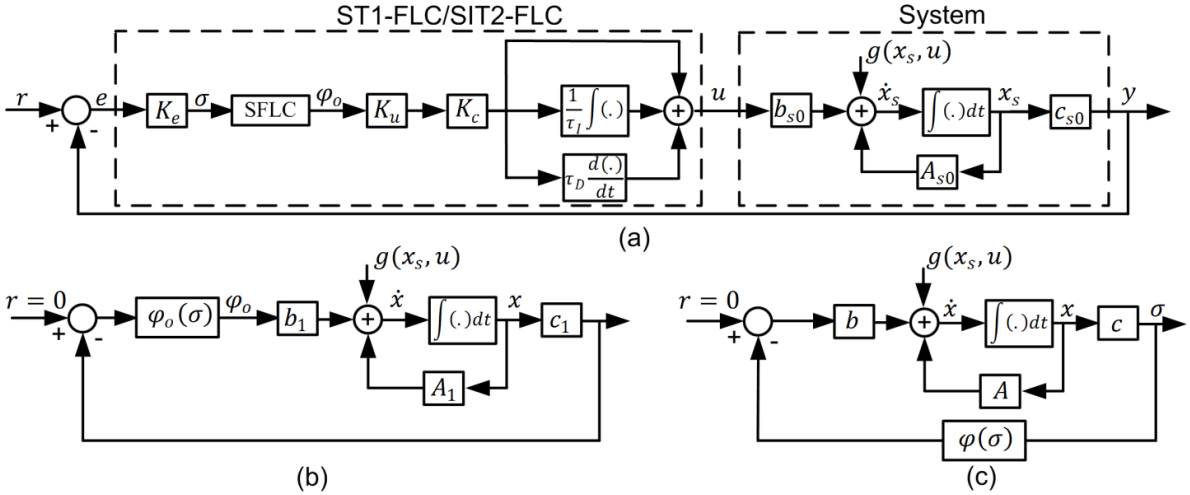

Fig.1. Illustration of the (a) SFLC control system (b) equivalent control system (c) Perturbed Lur'e system

The robust stability analysis of the fuzzy system is accomplished with respect to Theorem 1. Thus, at first an appropriate r value from the Popov plot of $G(jw)$ must be found such that (19) is satisfied. In other words, a slope r ($r > 0$) of a line that intercepts the point $-1/\bar{K} + j0$ must be obtained such that the Popov plot is always to the right to that line [44], [45]. After evaluating v and γ from (20), a symmetric positive-definite matrix W and a positive real number ε are selected to solve following Riccati equation:

$$A_r^T P + P A_r - P R_r P + Q_r = 0 \tag{25}$$

where

$$A_r = A - bv^T/\gamma \quad Q_r = \varepsilon W + vv^T/\gamma \quad R_r = -bb^T/\gamma \tag{26}$$

Once a positive-definite matrix P is calculated, a positive-definite matrix W_0 and an appropriate δ value is selected to obtain the robustness measure β. A relatively large β value corresponds to a potentiality more robust control system [44].

III. The Internal Structures of the SFLCS

Here, we will present internal structures of the ST1-FLC and SIT2-FLC to derive their FMs. It will be proven that Theorem-1 always holds for the handled SFLCs. Moreover, comparative explorations will be presented on the fundamental differences between the T1 and IT2 FMs.

A. Single Input Type-1 Fuzzy Logic Controllers

In this subsection, the ST1-FLC is presented to derive its FM and to present its properties. Moreover, theoretical explanations on tuning its design parameters will be provided.

1) Analytical derivations of the ST1-FLC

The rulebase of the handled ST1-FLC is as follows:

$$R^i\text{: IF } \sigma \text{ is } A_i \text{ THEN } \varphi_{o_{T1}} \text{ is } \varphi_i = B_i \tag{27}$$

where $i = -n, .., -1, 0, 1, ..., n$, B_i are crisp consequent MFs which satisfy $B_{-p} = -B_p, p = 1, ..., n$ and $B_0 = 0 < B_1 < \cdots < B_n = 1$ (as shown in Fig.2a); and A_i are the antecedent MFs defined with triangular T1-FSs as shown in Fig.2b (the bold lines). Here, c_i is the core of the MF that satisfies $c_{-p} = -c_p$ $(c_0 = 0, c_n = 1)$ and $0 < c_1 < \cdots < 1$. The total number of the rules (N) is defined as N=2n+1.

For a crisp input σ', the membership grades of the MFs are defined as:

$$\mu_{A_i}(\sigma') = \begin{cases} \dfrac{\sigma' - c_{i+1}}{c_i - c_{i+1}} & \sigma' \in [c_i, c_{i+1}] \\ \dfrac{c_{i-1} - \sigma'}{c_{i-1} - c_i} & \sigma' \in [c_{i-1}, c_i] \end{cases} \tag{28}$$

The corresponding output is defined as follows:

$$\varphi_{o_{T1}} = \frac{\sum_{i=1}^{N} \mu_{A_i}(\sigma') B_i}{\sum_{i=1}^{N} \mu_{A_i}(\sigma')} \tag{29}$$

Since it is always guaranteed that a crisp value of σ always belongs to two successive T1-FSs (i.e. A_i & A_{i+1}), the T1-FM for a generic input $\sigma \in [c_i, c_{i+1}]$ $(\varphi^i_{o_{T1}}(\sigma))$ can be derived as:

$$\varphi^i_{o_{T1}}(\sigma) = \frac{\mu_{A_i}(\sigma) B_i + \mu_{A_{i+1}}(\sigma) B_{i+1}}{\mu_{A_i}(\sigma) + \mu_{A_{i+1}}(\sigma)} \tag{30}$$

Substituting (28) into (30), we can obtain:

$$\varphi^i_{o_{T1}}(\sigma) = \frac{\left(\dfrac{\sigma - c_{i+1}}{c_i - c_{i+1}}\right) B_i + \left(\dfrac{c_i - \sigma}{c_i - c_{i+1}}\right) B_{i+1}}{\left(\dfrac{\sigma - c_{i+1}}{c_i - c_{i+1}}\right) + \left(\dfrac{c_i - \sigma}{c_i - c_{i+1}}\right)} \tag{31}$$

Then, (31) can be reformulated as:

$$\varphi^i_{o_{T1}}(\sigma) = k^i_{T1}\sigma + \eta^i_{T1} \tag{32}$$

where k^i_{T1} and η^i_{T1} are defined as:

$$k^i_{T1} = \frac{B_{i+1} - B_i}{c_{i+1} - c_i} \quad \eta^i_{T1} = \frac{B_i c_{i+1} - B_{i+1} c_i}{c_{i+1} - c_i} \tag{33}$$

Alike, the T1-FM for $\sigma \in [c_0, c_1]$ $(\varphi^{+0}_{o_{T1}}(\sigma))$ can be derived as:

$$\varphi^{+0}_{o_{T1}}(\sigma) = \sigma\, k^0_{T1} \tag{34}$$

where k^0_{T1} is:

$$k^0_{T1} = B_1/c_1 \tag{35}$$

It can be observed that the T1-FM reduces to a Linear Mapping (LM) for $\sigma \in [c_0, c_1]$

Theorem-2: Let $\varphi_{o_{T1}}(\sigma)$ denote the T1-FM. It holds that:

(i) $\varphi_{o_{T1}}(\sigma)$ is a symmetrical FM with respect to σ, i.e. $\varphi_{o_{T1}}(\sigma) = -\varphi_{o_{T1}}(-\sigma)$ for $\forall \sigma \neq 0$ and $\varphi_{o_{T1}}(0) = 0$.

(ii) $\varphi_{o_{T1}}(\sigma)$ is a continuous FM with regard to its input variable.

Proof: See Appendix A.

Theorem-3: The T1-FM always belongs to a sector $\left[K_{min_{T1}}, K_{max_{T1}}\right]$ for $\sigma \in [c_{-n}, c_n]$, such that:

$$K_{min_{T1}} \sigma^2 \leq \varphi_{o_{T1}} \sigma \leq K_{max_{T1}} \sigma^2 \tag{36}$$

where

$$K_{min_{T1}} \equiv \inf_{\substack{\sigma \in [c_{-n}, c_n] \\ i \in [-n, n]}} K^i_{min_{T1}} \quad K_{max_{T1}} \equiv \sup_{\substack{\sigma \in [c_{-n}, c_n] \\ i \in [-n, n]}} K^i_{max_{T1}} \tag{37}$$

Here, $K^i_{min_{T1}}$ and $K^i_{max_{T1}}$ are the sector bounds of $\varphi^i_{o_{T1}}(\sigma)$ and are defined for $i \neq 0$ as:

$$K^i_{min_{T1}} = \begin{cases} B_{i+1}/c_{i+1} & B_{i+1} > (B_i c_{i+1})/c_i \\ B_i/c_i & B_{i+1} < (B_i c_{i+1})/c_i \end{cases} \tag{38}$$

$$K^i_{max_{T1}} = \begin{cases} B_i/c_i & B_{i+1} > (B_i c_{i+1})/c_i \\ B_{i+1}/c_{i+1} & B_{i+1} < (B_i c_{i+1})/c_i \end{cases} \tag{39}$$

and for $i = 0$ as $K^0_{min_{T1}} = 0$ and $K^0_{max_{T1}} = B_1/c_1$.

Proof: See Appendix B.

Corollary-1

(i) Theorem 1 holds since the T1-FM is a symmetrical, continuous and sector bounded mapping.

(ii) The T1-FM can be represented in n $(i = 1, ..., n)$ multiple bends as follows:

$$\varphi_{o_{T1}}(\sigma) = \begin{cases} k^i_{T1}\sigma + \eta^i_{T1} & \sigma \in [c_i, c_{i+1}] \\ k^0_{T1}\sigma & \sigma \in [-c_1, c_1] \\ -\left(k^i_{T1}\sigma + \eta^i_{T1}\right) & \sigma \in [-c_{i+1}, -c_i] \end{cases} \tag{40}$$

where k^i_{T1}, η^i_{T1} and k^0_{T1} are given in (33) and (35).

2) Gain Analysis of the ST1-FLC structure

Here, the gain analysis of the ST1-FLC will be examined only for $\sigma \in [0, c_n]$, since $\varphi_{o_{T1}}(\sigma)$ is a symmetrical FM (Theorem 2), in comparison with the UM. Thus, let us first define:

$$v_o(\sigma) = \varphi_{o_{T1}}(\sigma) - \varphi_{o_{UM}}(\sigma) \tag{41}$$

Here, $v_o(\sigma)$ is defined as the difference between the T1-FM and UM. The variation of $v_o(\sigma)$ with respect to σ is as

$$\Delta v_o(\sigma) = \Delta v_o(\sigma)/\sigma \tag{42}$$

It can be observed from the sign variation of $\Delta v_o(\sigma)$:

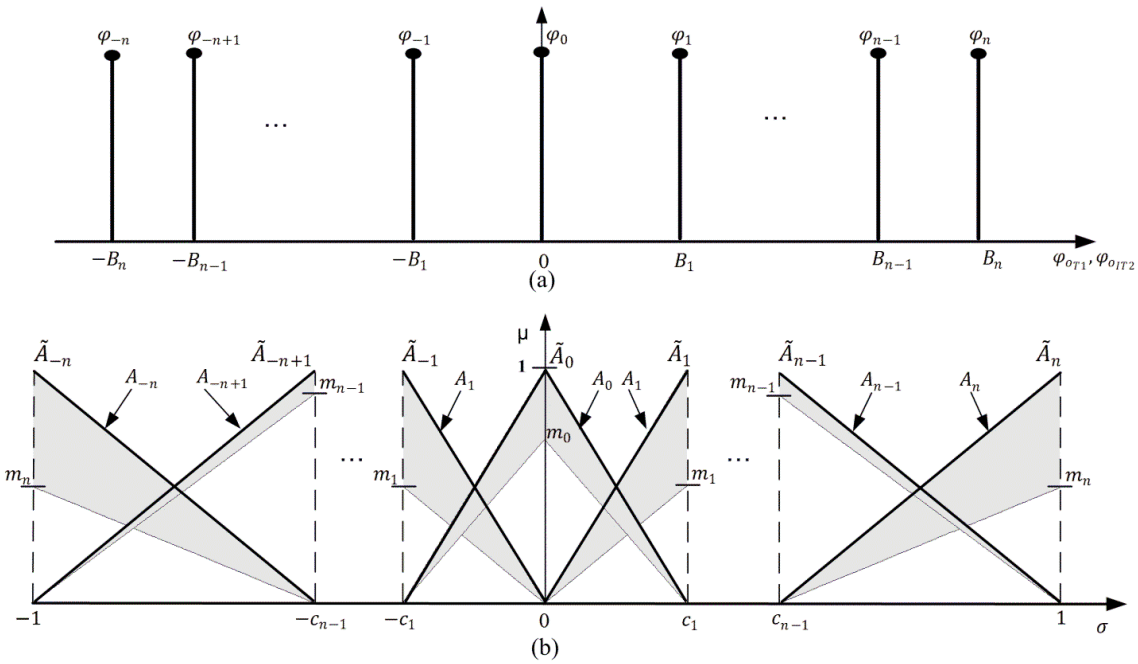

Fig. 2. Illustration of the (a) consequent MFs (b) antecedent MFs of the ST1-FLC and SIT2-FLC structures

- If $\Delta v_o > 0$, then the CA_{T1} is more aggressive in comparison to the UM's one for $\forall\sigma \in \mathbf{O_a}$
- If $\Delta v_o < 0$, then the CA_{T1} is smoother in comparison to the UM's one for $\forall\sigma \in \mathbf{O_s}$.

Here $\mathbf{O_a}$ and $\mathbf{O_s}$ indicate some neighborhoods in $[0, c_n]$. Thus, the sign variation of $\Delta v_o(\sigma)$ for $\sigma \in [0, c_1]$ and $\sigma \in [c_i, c_{i+1}]$ will be investigated to determine these regions.

For $\sigma \in [0, c_1]$, (42) becomes as follows:

$$\Delta v_o^0(\sigma) = X^0(\sigma)/Y^0(\sigma) = B_1/c_1 - 1 \quad (43)$$

In comparison to the UM, the following CA_{T1}s can be observed:

CA_{T1}(i): If $B_1/c_1 < 1$ then $\Delta v_o^0 < 0$ for $\forall\sigma \in \mathbf{O_s}$ where $\mathbf{O_s} \in [0, c_1]$. Thus, the CA_{T1} will be always smoother.

CA_{T1}(ii): If $B_1/c_1 > 1$ then $\Delta v_o^0 > 0$ for $\forall\sigma \in \mathbf{O_a}$ where $\mathbf{O_a} \in [0, c_1]$. Thus, the CA_{T1} will be always more aggressive.

For $\sigma \in [c_i, c_{i+1}]$, (42) becomes as follows:

$$\Delta v_o^i(\sigma) = \frac{B_{i+1}(c_i - \sigma) + B_i(\sigma - c_{i+1}) + \sigma(c_{i+1} - c_i)}{\sigma(c_i - c_{i+1})} \quad (44)$$
$$\Delta v_o^i(\sigma) = X^i(\sigma)/Y^i(\sigma)$$

To determine $\mathbf{O_a}$ and $\mathbf{O_s}$, the zero crossing point of $\Delta v_o^i(\sigma)$ ($X^i(\sigma) = 0$) is derived and found as:

$$\sigma_{X^i} = (B_i c_{i+1} - B_{i+1} c_i)/(B_i - B_{i+1} - c_i + c_{i+1}) \quad (45)$$

The point σ_{X^i} provides information about the sign variation of $\Delta v_o^i(\sigma)$. In comparison to the UM, it can be observed that:

CA_{T1}(iii):If $1 > B_i/c_i > 0$ and $1 > B_{i+1}/c_{i+1} > 0$, then $\Delta\varepsilon_o^i < 0$ for $\forall\sigma \in O_s$ where $\mathbf{O_s} \in [c_i, c_{i+1}]$. Thus, the CA_{T1} will be always smoother.

CA_{T1}(iv):If $B_i/c_i > 1$ and $B_{i+1}/c_{i+1} > 1$, then $\Delta v_o^i > 0$ for $\forall\sigma \in \mathbf{O_a}$ where $\mathbf{O_a} \in [c_i, c_{i+1}]$. Thus, the CA_{T1} will be always more aggressive.

CA_{T1}(v):If $B_i/c_i > 1 > B_{i+1}/c_{i+1} > 0$, then $\Delta v_o^i > 0$ for $\forall\sigma \in \mathbf{O_a}$ where $\mathbf{O_a} \in [c_i, \sigma_{X^i}]$ while $\Delta v_o^i < 0$ for $\forall\sigma \in \mathbf{O_s}$ where $\mathbf{O_s} \in [\sigma_{X^i}, c_{i+1}]$. Thus, the CA_{T1} will be smoother for $\sigma \in \mathbf{O_s}$ while more aggressive for $\sigma \in \mathbf{O_a}$.

CA_{T1}(vi):If $B_{i+1}/c_{i+1} > 1 > B_i/c_i > 0$, then $\Delta v_o^i > 0$ for $\forall\sigma \in \mathbf{O_a}$ where $\mathbf{O_a} \in [\sigma_{X^i}, c_{i+1}]$ while $\Delta v_o^i < 0$ for $\forall\sigma \in \mathbf{O_s}$ where $\mathbf{O_s} \in [c_i, \sigma_{X^i}]$. Thus, the CA_{T1} will be always smoother for $\sigma \in \mathbf{O_s}$ while more aggressive for $\sigma \in \mathbf{O_a}$.

Note that; if $B_1/c_1 = B_{i+1}/c_{i+1} = \cdots = B_n/c_n = 1$, then the FM will reduce to a UM since $\Delta v_o = 0$.

B. Single Input Interval Type-2 Fuzzy Logic Controllers

In this subsection, the SIT2-FLC is presented to derive its FM and to present its properties. Moreover, theoretical explanations on tuning the size of the FOU will be provided.

1) Analytical derivations of the ST2-FLC

The rule structure of the SIT2-FLC is as follows:

$$R^i\text{: IF } \sigma \text{ is } \tilde{A}_i \text{ THEN } \varphi_{o_{IT2}} \text{ is } \varphi_i = B_i \quad (46)$$

where B_i are crisp consequent MFs (the same consequents of its T1 counterpart). The antecedent parts of the rules are defined with triangular IT2-FSs $\tilde{A}_i$ which are constructed by extending the T1-FSs as shown in Fig.2b. The IT2-FSs are described in terms of Upper MFs (UMFs) ($\overline{\mu}_{\tilde{A}_i}$) and Lower MFs (LMFs) ($\underline{\mu}_{\tilde{A}_i}$) which are defined with their cores (c_i) and the height of their LMFs (m_i). In this study, the cores of the LMFs and UMFs will be defined with the identical core values of its T1 counterpart. Thus, the heights of the LMFs m_i are the only parameters which create the FOU in IT2-FSs and are the only design parameters to be tuned. The heights of the LMFs satisfy $m_{-p} = m_p (p = 1, \ldots, n)$ to have uniformly distributed symmetrical LMFs. The total number of the rules is N=2n+1.

For a crisp input σ', the UMFs are defined as in (28) while the LMFs are defined as:

$$\underline{\mu}_{\tilde{A}_i}(\sigma') = m_i\, \overline{\mu}_{\tilde{A}_i}(\sigma') \quad (47)$$

The corresponding SIT2-FLC output is defined as follows:

$$\varphi_{o_{IT2}} = \left(\varphi^r_{o_{IT2}} + \varphi^l_{o_{IT2}}\right)/2 \quad (48)$$

where φ^r_o and φ^l_o are the end points of the type reduced set which are defined as follows:

$$\varphi^r_{o_{IT2}} = \frac{\sum_{i=1}^{R} \underline{\mu}_{\tilde{A}_p}(\sigma')B_p + \sum_{R+1}^{N} \overline{\mu}_{\tilde{A}_p}(\sigma')B_p}{\sum_{i=1}^{R} \underline{\mu}_{\tilde{A}_p}(\sigma') + \sum_{R+1}^{N} \overline{\mu}_{\tilde{A}_p}(\sigma')} \quad (49)$$

$$\varphi^l_{o_{IT2}} = \frac{\sum_{p=1}^{L} \overline{\mu}_{\tilde{A}_p}(\sigma')B_p + \sum_{L+1}^{N} \underline{\mu}_{\tilde{A}_p}(\sigma')\,B_p}{\sum_{i=1}^{L} \overline{\mu}_{\tilde{A}_p}(\sigma') + \sum_{L+1}^{N} \underline{\mu}_{\tilde{A}_p}(\sigma')} \quad (50)$$

where R and L are the switching points [26]. As shown in Fig.2b, the SIT2-FLC employs fully overlapping IT2-FSs in the sense of LMFs and UMFs. Hence, it is guaranteed that a crisp value σ' always belongs to two successive IT2-FSs ($\tilde{A}_i$ & $\tilde{A}_{i+1}$). Thus, since only N=2 rules will be always activated, the values of R and L are equal to 1 [43]. This gives the opportunity to derive the IT2-FM in a closed form. The IT2-FM for an input $\sigma \in [c_i, c_{i+1}]$ $\left(\varphi^i_{o_{IT2}}(\sigma)\right)$ is derived as:

$$\varphi^i_{o_{IT2}}(\sigma) = \frac{1}{2}\left(\frac{\overline{\mu}_{\tilde{A}_i}(\sigma)B_i + \underline{\mu}_{\tilde{A}_{i+1}}(\sigma)B_{i+1}}{\overline{\mu}_{\tilde{A}_i}(\sigma) + \underline{\mu}_{\tilde{A}_i}(\sigma)} + \frac{\underline{\mu}_{\tilde{A}_i}(\sigma)B_i + \overline{\mu}_{\tilde{A}_{i+1}}(\sigma)B_{i+1}}{\underline{\mu}_{\tilde{A}_i}(\sigma) + \overline{\mu}_{\tilde{A}_{i+1}}(\sigma)}\right) \quad (51)$$

Substituting the UMF and LMF values given in (28) and (47) into (51), we can formulate:

$$\varphi^i_{o_{IT2}}(\sigma) = k^i_{IT2}(\sigma)\,\sigma + \eta^i_{IT2}(\sigma) \quad (52)$$

where $k^i_{IT2}(\sigma)$ is defined as:

$$k^i_{IT2}(\sigma) = \frac{1}{2}\left(\frac{B_{i+1} - B_i m_i}{c_{i+1}m_i - c_i + \sigma(-m_i + 1)} + \frac{B_i - B_{i+1}m_{i+1}}{c_i m_{i+1} - c_{i+1} + \sigma(-m_{i+1} + 1)}\right) \quad (53)$$

and $\eta^i_{IT2}(\sigma)$ is defined as:

$$\eta^i(\sigma) = \frac{1}{2}\left(\frac{B_{i+1}c_i - B_i c_{i+1}m_i}{-c_{i+1}m_i + c_i + \sigma(m_i - 1)} + \frac{B_i c_{i+1} - B_{i+1}c_i m_{i+1}}{-c_i m_{i+1} + c_{i+1} + \sigma(m_{i+1} - 1)}\right) \quad (54)$$

Similarly, the IT2-FM for $\sigma \in [0, c_1]$ $(\varphi^{+0}_{o_{IT2}}(\sigma))$ is derived as:

$$\varphi^{+0}_{o_{IT2}}(\sigma) = k^0_{IT2}(\sigma)\,\sigma \quad (55)$$

where $k^0_{IT2}(\sigma)$ is:

$$k^0_{IT2}(\sigma) = \frac{1}{2}\left(\frac{B_1}{\sigma - \sigma m_0 + c_1 m_0} - \frac{B_1 m_1}{\sigma - c_1 - \sigma m_1}\right) \quad (56)$$

Reminding that for $\sigma \in [0, c_1]$ the T1-FM reduced to a LM, it can be seen that the IT2-FM results with a nonlinear mapping which shows the effect of the FOU on the FM generation.

Theorem-4: Let $\varphi_{o_{IT2}}(\sigma)$ denote the FM of the SIT2-FLC.

(i) $\varphi_{o_{IT2}}(\sigma)$ is a symmetrical FM with respect to σ, i.e. $-\varphi_{o_{IT2}}(\sigma) = \varphi_{o_{IT2}}(-\sigma)$ for $\forall\sigma \neq 0$ and $\varphi_{o_{IT2}}(0) = 0$.

(ii) $\varphi_{o_{IT2}}(\sigma)$ is a continuous FM with regard to its input variable σ.

Proof: See Appendix C.

Theorem-5: The IT2-FM always belongs to a bounded sector $\left[K_{min_{IT2}}, K_{max_{IT2}}\right]$ for $\sigma \in [c_{-n}, c_n]$ such that:

$$K_{min_{IT2}}\sigma^2 \leq \varphi_{o_{IT2}}\,\sigma \leq K_{max_{IT2}}\sigma^2, \forall\sigma \neq 0 \quad (57)$$

where

$$K_{min_{IT2}} \equiv \inf_{\substack{\sigma\in[c_{-n},c_n]\\ i\in[-n,n]}} K^i_{min_{IT2}}\ K_{max_{IT2}} \equiv \sup_{\substack{\sigma\in[c_{-n},c_n]\\ i\in[-n,n]}} K^i_{max_{IT2}} \quad (58)$$

$K^i_{min_{IT2}}$ and $K^i_{max_{IT2}}$ are the sector bounds of $\varphi^i_{o_{IT2}}(\sigma)$ and are defined as:

$$K^i_{min_{IT2}}\sigma^2 \leq \varphi^i_{o_{IT2}}\sigma \leq K^i_{max_{IT2}}\sigma^2, \forall\sigma \neq 0 \quad (58)$$

Here, $K^i_{min_{IT2}}$ and $K^i_{max_{IT2}}$ will map to different values with respect to m_i and m_{i+1} values.

Proof: See Appendix D.

Corollary-2

(i) Theorem 1 holds since the IT2-FM is a symmetrical, continuous and sector bounded mapping.

(ii) The IT2-FM can be represented in n multiple bends as:

$$\varphi_{o_{IT2}}(\sigma) = \begin{cases} k^i_{IT2}(\sigma)\sigma + \eta^i_{IT2}(\sigma) & \sigma \in [c_i, c_{i+1}] \\ k^0_{IT2}(\sigma)\,\sigma & \sigma \in [-c_1, c_1] \\ -k^i_{IT2}(\sigma)\sigma - \eta^i_{IT2}(\sigma) & \sigma \in [-c_{i+1}, -c_i] \end{cases} \quad (60)$$

where $k^i_{IT2}(\sigma), \eta^i_{IT2}(\sigma)$ and $k^0_{IT2}(\sigma)$ are defined in (53), (54) and (56), respectively.

2) Gain analysis of the SIT2-FLC structure

The gain analysis of the SIT2-FLC will be examined only for $[0, c_n]$, since $\varphi_{o_{IT2}}(\sigma)$ is a symmetrical FM (Theorem 4), in comparison with the T1-FM. In this context, let us first define:

$$\varepsilon_0(\sigma) = \varphi_{o_{IT2}}(\sigma) - \varphi_{o_{T1}}(\sigma) \quad (61)$$

where $\varepsilon_0(\sigma)$ is defined as the difference between the T1-FM and IT2-FM. Then, the gain variation of $\varepsilon_0(\sigma)$ with respect to σ can be defined as:

$$\Delta\varepsilon_0(\sigma) = \varepsilon_0(\sigma)/\sigma \quad (62)$$

It can be observed from the sign variation of $\Delta\varepsilon_0(\sigma)$:

- If $\Delta\varepsilon_0 > 0$, then the CA_{IT2} is more aggressive in comparison with the CA_{T1} for $\forall\sigma \in \mathbf{O_a}$.
- If $\Delta\varepsilon_0 < 0$, then the CA_{IT2} is smoother in comparison with the CA_{T1} for $\forall\sigma \in \mathbf{O_s}$.

The neighborhoods $\mathbf{O_a}$ $(\Delta\varepsilon^0_o > 0)$ and $\mathbf{O_s}(\Delta\varepsilon^0_o < 0)$ can be determined by simply investigating the zero crossing points of $\Delta\varepsilon_0(\sigma)$. Thus, the sign variation of $\Delta\varepsilon_0(\sigma)$ will be examined with respect to the parameters m_i, m_{i+1} for $\sigma \in [0, c_1]$ and $\sigma \in [c_i, c_{i+1}]$.

For $\sigma \in [0, c_1]$, to determine $\mathbf{O_a}$ and $\mathbf{O_s}$, the zero crossing points of $\Delta\varepsilon^0_o(\sigma)$ (given in (D.4)) are found as:

$$\sigma_{P^0_1} = c_1 \quad \sigma_{P^0_2} = \frac{c_1(1 + m_0(m_1 - 2))}{2(m_0 - 1)(m_1 - 1)} \quad (63)$$

Here, $\sigma_{P^0_1}$ is one of the boundary points of the interval $\sigma \in [0, c_1]$. Thus, the IT2-FM will reduce to its T1 counterpart at the point c_1 since $\Delta\varepsilon^0_o = 0$. Whereas the point $\sigma_{P^0_2}$ will provide information about sign variation of $\Delta\varepsilon^0_o(\sigma)$. The following CA_{IT2}s, in comparison to the CA_{T1}, can be observed:

CA_{IT2}(i):If $0 < m_1 \leq 1$ and $m_{0_1} \leq m_0 < 1$, then $\Delta\varepsilon^0_o < 0$ for $\forall\sigma \in \mathbf{O_s}$ where $\mathbf{O_s} \in [0, c_1)$ and $m_{0_1} = 1/(2 - m_1)$. Thus, the CA_{IT2} will be always smoother.

CA_{IT2}(ii):If $1/2 \leq m_1 < 1$ and $0 < m_0 \leq m_{0_2}$, then $\Delta\varepsilon^0_o > 0$ for $\forall\sigma \in \mathbf{O_a}$ where $\mathbf{O_a} \in [0, c_1)$ and $m_{0_2} = (2m_1 - 1)/m_1$.Thus, the CA_{IT2} will be always more aggressive.

CA_{IT2}(iii):If $\left\{\begin{array}{c} 0<m_1\le 1/2 \text{ and } 0\le m_0<m_{0_1} \\ \text{or} \\ 1/2\le m_1<1 \text{ and } m_{0_2}<m_0\le m_{0_1}\end{array}\right\}$, then $\Delta\varepsilon_o^0>0$ for $\forall\sigma\in\left(0,\sigma_{P_2^0}\right)$ while $\Delta\varepsilon_o^0<0$ for $\forall\sigma\in\left(\sigma_{P_2^0},c_1\right)$. Thus, the CA_{IT2} will be always smoother for $\sigma\in\mathbf{O_s}$ $(\mathbf{O_s}\in(0,\sigma_{P_2^0}))$ while more aggressive for $\sigma\in\mathbf{O_a}$ $(\mathbf{O_a}\in(\sigma_{P_2^0},c_1))$.

For $\sigma\in[c_i,c_{i+1}]$, the roots of $P^i(\sigma)$ (presented in (D.14)) are found as $\sigma_{P_1^i}=c_i$, $\sigma_{P_2^i}=c_{i+1}$ and

$$\sigma_{P_3^i}=\frac{(c_{i+1}+c_i)(1+(m_i-2)m_{i+1})}{2(m_i-1)(m_{i+1}-1)} \quad (64)$$

The $\sigma_{P_1^i}$ and $\sigma_{P_2^i}$ are the boundary points of the interval $[c_i,c_{i+1}]$. So, the IT2-FM will always reduce to its T1 counterpart at its boundary points since $\Delta\varepsilon_o^i=0$. Here, $\sigma_{P_3^i}$ will provide information about sign variation of $\Delta\varepsilon_o^i(\sigma)$. In comparison to the CA_{T1}, it can be observed that:

CA_{IT2}(iv):If $0<m_{i+1}<1$ and $m_{i_1}\le m_i<1$, then $\Delta\varepsilon_o^i<0$ for $\forall\sigma\in\mathbf{O_s}$ where $\mathbf{O_s}=[c_i,c_{i+1}]$ and $m_{i_1}=1/(2-m_{i+1})$.So, the CA_{IT2} will be always smoother.

CA_{IT2}(v):If $1/2<m_{i+1}<1$ and $0<m_i<m_{i_2}$, then $\Delta\varepsilon_o^i>0$ for $\forall\sigma\in\mathbf{O_a}$ where $\mathbf{O_a}\in[c_i,c_{i+1}]$ and $m_{i_2}=(2m_{i+1}-1)/m_{i+1}$. Thus, the CA_{IT2} will be more aggressive.

CA_{IT2}(vi):If $\left\{\begin{array}{c} 0<m_{i+1}\le 1/2 \text{ and } 0\le m_i\le m_{i_1} \\ \text{or} \\ 1/2\le m_{i+1}<1 \text{ and } m_{i_2}\le m_i<m_{i_1}\end{array}\right\}$, then $\Delta\varepsilon_o^i>0$ for $\forall\sigma\in[c_i,\sigma_{P_3^i}]$ while $\Delta\varepsilon_o^0<0$ for $\forall\sigma\in[\sigma_{P_3^i},c_{i+1}]$. Thus, the CA_{IT2} will always be more aggressive for $\sigma\in\mathbf{O_a}(\mathbf{O_a}\in[c_i,\sigma_{P_3^i})$ while smoother for $\sigma\in\mathbf{O_s}$ $(\mathbf{O_s}\in[\sigma_{P_3^i},c_{i+1}])$.

IV. Design Methods for SFLCs

Here, we will present analytical design methods for the SFLCs composed of 3 and 5 rules on the analysis given in the preceding section. We will employ c_n=1 since the input domain is defined as [-1,1] and handle only the interval [0,1] since both FMs are symmetrical. It is worth to mention that the presented design methods can be also extended to SFLC of N>5 rules since the FMs can be presented in n multiple bends.

A. Design Methods for SFLCs composed of 3 rules

In this subsection, we will use the CAs to design the CCs of the SFLCs composed of 3 Rules (CC^{3R}s). In this structure, only one CA can be defined for the interval [0,1] since n=1.

In the design of the ST1-FLC, there is only one design parameter to be determined which is B_1 since we will employ B_0=c_0=0 and c_1=1. In this structure, only the CA_{T1}(i) and the CA_{T1}(ii) can be used to design the T1 fuzzy CC^{3R}s $\left(CC_{T1}^{3R}s\right)$. In comparison to CC of the UM (U-CC), to generate:

- a Smoother $CC_{T1}^{3R}\left(S\text{-}CC_{T1}^{3R}\right)$, then B_1 must be tuned according to the CA_{T1}(i).
- an Identical $CC_{T1}^{3R}\left(I\text{-}CC_{T1}^{3R}\right)$, then B_1 must be set to "1".
- a more Aggressive $CC_{T1}^{3R}\left(A\text{-}CC_{T1}^{3R}\right)$, then B_1 must be tuned according to the CA_{T1}(ii).

For the Parameter Settings (PSs) tabulated in Table I, the $S\text{-}CC_{T1}^{3R}$, $I\text{-}CC_{T1}^{3R}$ and $A\text{-}CC_{T1}^{3R}$ are generated and illustrated in Fig.3a, Fig.4a and Fig.5a, respectively and their corresponding gain variations $(\varphi_o(\sigma)/\sigma)$ are given in Fig.3b, Fig.4b and Fig.5b, respectively. Here, the U-CC and its gain variation are shown for comparison.

The design of the SIT2-FLC is accomplished as an extension of its T1 counterpart. Thus, the parameters B_1, B_0, c_1 and c_0 are set and fixed to the same values of the ST1-FLC. Thus, we have to tune only the FOU parameters (m_0,m_1). The CA_{IT2}(i), (ii) and (iii) can be used to design the IT2 fuzzy CC^{3R}s $\left(CC_{IT2}^{3R}s\right)$. In comparison to its T1 counterpart, to generate:

- a Smoother $CC_{IT2}^{3R}\left(S\text{-}CC_{IT2}^{3R}\right)$, then ($m_0$,$m_1$) must be tuned according to the CA_{IT2} (i).
- an Aggressive $CC_{IT2}^{3R}\left(A\text{-}CC_{IT2}^{3R}\right)$, then ($m_0$,$m_1$) must be tuned according to the CA_{IT2} (ii).
- an Inverse S-Shaped $CC_{IT2}^{3R}\left(ISS\text{-}CC_{IT2}^{3R}\right)$,then ($m_0$,$m_1$) must be tuned according to the CA_{IT2}(iii).

For the FOU parameters (m_0=0.9, m_1=0.2), (m_0=0.2, m_1=0.9) and (m_0=0.2, m_1=0.2), a $S\text{-}CC_{IT2}^{3R}$, an $A\text{-}CC_{IT2}^{3R}$ and an $ISS\text{-}CC_{IT2}^{3R}$ can be generated, respectively. Since B_1, B_0, c_1 and c_0 are fixed to the same values of their T1 counterparts, the $S\text{-}CC_{IT2}^{3R}$, $A\text{-}CC_{IT2}^{3R}$ and $ISS\text{-}CC_{IT2}^{3R}$ are shown with respect to the values of B_1=0.5, 1.0 and 1.8 in Fig.3a, Fig.4a and Fig.5a while their gain variations are in Fig.3b, Fig.4b and Fig.5b, respectively. The PSs of the SIT2-FLCs are given in Table I.

TABLE I. The PSs (B_0, m_0, m_1) of the SFLCs Presented in Fig. 3-5

Fig.3		Fig.4		Fig.5	
CC^{3R}	PS-1	CC^{3R}	PS-2	CC^{3R}	PS-3
$S\text{-}CC_{T1}^{3R}$	(0.5, −, −)	$I\text{-}CC_{T1}^{3R}$	(1.0, −, −)	$A\text{-}CC_{T1}^{3R}$	(1.8, −, −)
$S\text{-}CC_{IT2}^{3R}$	(0.5,0.9,0.2)	$S\text{-}CC_{IT2}^{3R}$	(1.0,0.9,0.2)	$S\text{-}CC_{IT2}^{3R}$	(1.8,0.9,0.2)
$A\text{-}CC_{IT2}^{3R}$	(0.5,0.2,0.9)	$A\text{-}CC_{IT2}^{3R}$	(1.0,0.2,0.9)	$A\text{-}CC_{IT2}^{3R}$	(1.8,0.2,0.9)
$ISS\text{-}CC_{IT2}^{3R}$	(0.5,0.2,0.2)	$ISS\text{-}CC_{IT2}^{3R}$	(1.0,0.2,0.2)	$ISS\text{-}CC_{IT2}^{3R}$	(1.8,0.2,0.2)

*In all CC^{3R}s, $B_0=c_0=0$, $c_1=1$

It can be observed that, since all T1-FMs reduce to LMs, the ST1-FLCs were only to generate linear CCs and thus resulted with constant gain variations as shown in Fig.3b-4b-5b. On the other hand, tuning the size of the FOU gave the opportunity to the SIT2-FLC (which have the identical B_1, B_0, c_1 and c_0 values) to implement commonly employed CCs as a result of their nonlinear gain variations shown in Fig.3-5. The presented CCs coincide with the derivations and analyses presented in the section III. Especially, from the results presented in Fig.4, the effect of FOU on the CC generation can be clearly observed. Since the parameter B_1 is set to "1", the T1-FM reduces to the UM and thus the ST1-FLC was able to only generate a U-CC while the SIT2-FLC was able to generate the $S\text{-}CC_{IT2}^{3R}$, $A\text{-}CC_{IT2}^{3R}$ and $ISS\text{-}CC_{IT2}^{3R}$. It can be concluded that the CC_{IT2}^{3R}s cannot be generated by ST1-FLCs. It is worth to mention that all SIT2-FLCs reduced to their T1 counterparts at the value c_1 since $\Delta\varepsilon_o^0=0$.

B. Design Methods for SFLCs composed of 5 rules

We will use the CAs to design the CCs of the SFLCs of 5 Rules (CC^{5R}s). Here, since n=2, the interval [0,1] is partitioned

into two subintervals, i.e. $[0,c_1]\cup[c_1,1]$. Thus, for each subinterval a CA must be defined, i.e. two CAs.

In the design of the ST1-FLC, the parameters to be tuned are B_1, c_1, B_2 since $B_0=c_0=0$ and $c_2=1$. In the design of the T1 fuzzy CC^{5R}s $\left(CC_{T1}^{5R}s\right)$, the CA_{T1}(i) and the CA_{T1}(ii) can be used for the interval $[0, c_1]$ whereas for the interval $[c_1,1]$ the CA_{T1}(iii), CA_{T1}(iv), CA_{T1}(v) and CA_{T1} (vi) can be employed. Thus, in comparison to a UM, to generate:

- a Smoother CC_{T1}^{5R} $\left(S\text{-}CC_{T1}^{5R}\right)$, then B_1 and c_1 must be according to CA_{T1}(i) while B_2, B_1 and c_1 must be according to CA_{T1}(iii). For instance, by setting (B_2, B_1, c_1) = (0.5, 0.8, 1.0).
- an Identical CC_{T1}^{5R} $\left(I\text{-}CC_{T1}^{5R}\right)$, then the parameters must be set as B_2=1, B_1=0.5 and c_1=0.5.
- an Aggressive CC_{T1}^{5R} $\left(A\text{-}CC_{T1}^{5R}\right)$ when B_1 and c_1 must be set according to CA_{T1}(ii) while B_2, B_1 and c_1 must be set according to CA_{T1}(iv). For instance, by setting (B_2, B_1, c_1) = (0.6, 0.3, 1.0).

For the PSs given in Table II, the $S\text{-}CC_{T1}^{5R}$, $I\text{-}CC_{T1}^{5R}$ and $A\text{-}CC_{T1}^{5R}$ are generated and shown in Fig.6.

In the design of the SIT2-FLC, the parameters B_2, c_2, B_1, c_1, B_0 and c_0 are set and fixed to the same values of its T1 counterpart. Thus, the design parameters of the SIT2-FLC to be tuned are only the FOU parameters m_0, m_1 and m_2. In the design of the IT2 fuzzy CC^{5R}s $\left(CC_{IT2}^{5R}s\right)$, the CA_{IT2}(i), CA_{IT2}(i) and CA_{IT2} (iii) can be used for the interval $[0,c_1]$, whereas for interval $[c_1,1]$ the CA_{IT2}(iv), CA_{IT2}(v) and CA_{IT2}(vi) can be employed. In comparison to its T1-FM, to generate:

- a Smoother $CC_{IT2}^{5R}\left(S\text{-}CC_{IT2}^{5R}\right)$, then m_0 and m_1 must be set according to CA_{IT2}(i) while m_1 and m_2 must be set according to CA_{IT2}(iv). For instance, by setting (m_0, m_1, m_2) = (0.9, 0.5, 0.1).
- an Aggressive $CC_{IT2}^{5R}\left(A\text{-}CC_{IT2}^{5R}\right)$, then m_0 and m_1 must be set according to CA_{IT2} (ii) while m_1 and m_2 must be set according to CA_{IT2}(v). For instance, by setting (m_0, m_1, m_2) = (0.1,0.5,0.9).
- an S-Shaped $CC_{IT2}^{5R}\left(SS\text{-}CC_{IT2}^{5R}\right)$, then m_0 and m_1 must be set according to CA_{IT2}(i) while m_1 and m_2 must be set according to CA_{IT2}(v). For instance, by setting (m_0, m_1, m_2) = (0.9 ,0.1, 0.9).

In Fig.6, the $S\text{-}CC_{IT2}^{5R}$, $A\text{-}CC_{IT2}^{5R}$ and $SS\text{-}CC_{IT2}^{5R}$ are illustrated with respect to their T1 counterparts since the generation of the CC_{IT2}^{5R}s is accomplished as an extension of the CC_{T1}^{5R}s. The PSs of the sketched CC_{IT2}^{5R}s are presented in Table II.

Firstly, it is worth to mention that the 5 rule based SIT2-FLC gave the opportunity to generate an S-shaped CC which could not be generated by its 3 rule based IT2 counterpart.

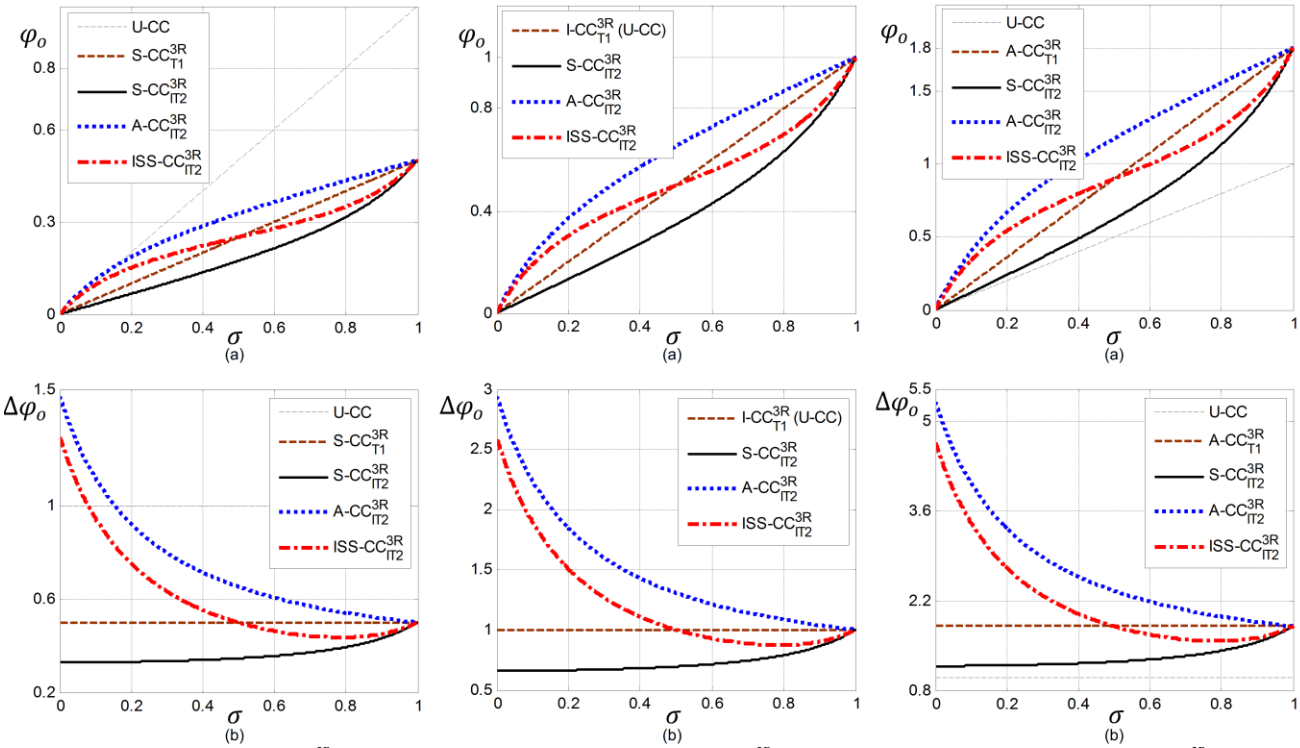

Fig.3 Illustration of the (a) CC^{3R}s and (b) $\varphi_o(\sigma)\ /\sigma$ for PS-1

Fig.4. Illustration of the (a) CC^{3R}s and (b) $\varphi_o(\sigma)\ /\sigma$ for PS-2

Fig.5. Illustration of the (a) CC^{3R}s and (b) $\varphi_o(\sigma)\ /\sigma$ for PS-3

TABLE II. THE PSS (B_1, C_1, B_2, m_0, m_0, m_1, m_2) OF THE SFLCS PRESENTED IN FIG. 6

Fig.6a		Fig.6b		Fig.6c	
CC^{5R}	PS-4	CC^{5R}	PS-5	CC^{5R}	PS-6
$S\text{-}CC_{T1}^{5R}$	(0.5,0.8,1.0, −, −, −)	$A\text{-}CC_{T1}^{5R}$	(0.6,0.3,1.0, −, −, −)	$I\text{-}CC_{T1}^{5R}$	(0.5,0.5,1.0, −, −, −)
$S\text{-}CC_{IT2}^{5R}$	(0.5,0.8,1.0,0.9,0.5,0.1)	$S\text{-}CC_{IT2}^{5R}$	(0.6,0.3,1.0,0.9,0.5,0.1)	$S\text{-}CC_{IT2}^{5R}$	(0.5,0.5,1.0,0.9,0.5,0.1)
$A\text{-}CC_{IT2}^{5R}$	(0.5,0.8,1.0,0.1,0.5,0.9)	$A\text{-}CC_{IT2}^{5R}$	(0.6,0.3,1.0,0.1,0.5,0.9)	$A\text{-}CC_{IT2}^{5R}$	(0.5,0.5,1.0,0.1,0.5,0.9)
$SS\text{-}CC_{IT2}^{5R}$	(0.5,0.8,1.0,0.9,0.1,0.9)	$SS\text{-}CC_{IT2}^{5R}$	(0.6,0.3,1.0,0.9,0.1,0.9)	$SS\text{-}CC_{IT2}^{5R}$	(0.5,0.5,1.0,0.9,0.1,0.9)

*In all CC^{5R}s, $B_0 = c_0 = 0$, $c_2 = 1$

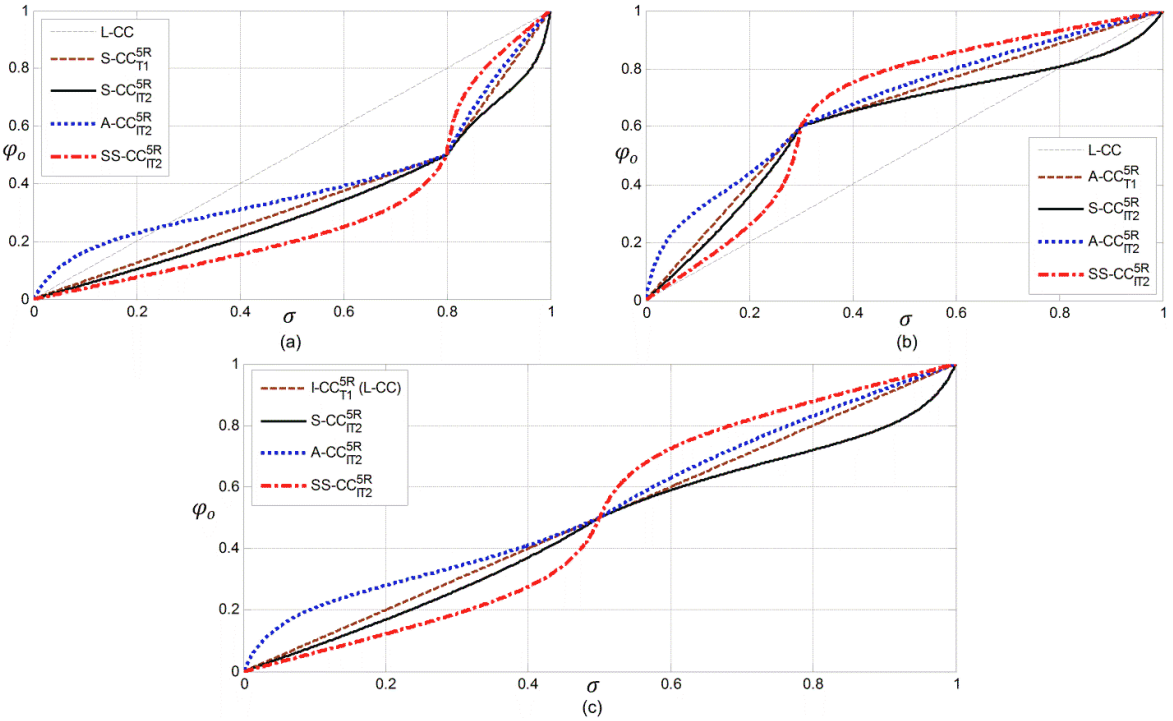

Fig.6. Illustration of the CC^{5R}s for the (a) PS-4 (b) PS-5 (c) PS-6

It can be also observed that the all IT2-FMs reduce to their T1 counterpart at their boundary points (c_1 and 1) which coincide with the presented derivations. Similar to the presented CC^{3R}s; it can be seen that the SIT2-FLC is able to implement CCs which have relatively higher input sensitivity than their T1 counterparts. Especially, from the results presented in Fig.6c (the T1-FM reduces to the UM), the effect of the FOU on the CC generation is clearly demonstrated. For this setting, the SIT2-FLC was able generate an SS-CC$^{5R}_{IT2}$ (beside a S-CC$^{5R}_{IT2}$ and an A-CC$^{5R}_{IT2}$) by simply tuning the size of the FOU. This shows clearly the design simplicity of the SIT2-FLCs. It can be seen that the CC$^{5R}_{IT2}$s cannot be duplicated by the ST1-FLCs.

Remark-1: In the design of the 5 rule based SFLCs, there are common design parameters (B_1 and c_1, for the ST1-FLC and m_1 for the SIT2-FLC) which affect the CAs in both intervals, $[0,c_1]$ and $[c_1,1]$. Thus, an independent CA tuning for each subinterval is not possible. Hence, it is suggested to tune firstly the parameters for the interval $[0,c_1]$ and then to design a CA for the interval $[c_1,1]$ since the CA around the origin ($[0,c_1]$) can directly affect the robustness of the system [28].

Remark-2: It should be noted that various types of CCs can be generated by employing different combinations of the CAs for both the SFLCs. In this paper, only design methods for generating commonly employed CCs such as smooth, aggressive, S-shaped are presented due to limited space.

V. Illustrative Studies: Control Curve and Robust Control Performance

We will illustrate the proposed design methods and robust stability analyses. As it has been shown in the section IV, the FOU of the SIT2-FLC gives the opportunity to generate CCs which cannot be generated by ST1-FLCs which are composed of the 3 or 5 rules. In this context, it will be firstly investigated whether the CC$^{3R}_{IT2}$s can be duplicated with various ST1-FLCs. Then, the robust control performances of the fuzzy systems are examined on a benchmark system. The studies were done on a personal computer with an Intel Core I5 1.61 GHz processor, 4 GB RAM and using MATLAB/Simulink 7.4.0.

A. Control Curve Comparison of the SFLCs

Here, it will be firstly examined whether increasing the number of rules of ST1-FLC will give the opportunity to duplicate the IT2-FM. Then, it will investigated whether it is possible construct identical IT2-FMs by employing different types of antecedent and consequent MFs to the ST1-FLCs. Increasing the number of rules and/or employing different types of MFs will naturally increase the degree of freedom of the ST1-FLCs. Firstly, we will design three SIT2-FLCs composed of only 3 rules with setting B_0=c_0=0 and B_1=c_1=1. Then, by simply tuning the size of the FOU, three CC$_{IT2}$s are constructed which are a S-CC$^{3R}_{IT2}$ (m_0=0.9,m_1=0.2), an A-CC$^{3R}_{IT2}$ (m_0=0.2,m_1=0.9) and an ISS-CC$^{3R}_{IT2}$ (m_0=0.2, m_1=0.2) that are shown in Fig.4a (for the interval [0,1]). The sector bounds $K_{min_{IT2}}$ and $K_{max_{IT2}}$ of the SIT2-FLCs are calculated via Table A (presented in the Appendix D) and are tabulated in Table III. To compare the matching performance of T1-FMs, the input and output data of each designed SIT2-FLC is collected with a sampling magnitude of 0.001. The performances of the T1-FMs are measured and compared via:

$$IAE = \sum_{k=1}^{2001} \varepsilon[k] \tag{65}$$

where $\varepsilon[k]$ is defined as $\varepsilon[k] = \left|\varphi_{o_{IT2}}[k] - \varphi_{o_{T1}}[k]\right|$ at the k^{th} sample. Moreover, the sector bounds of the ST1-FLCs are examined in comparison to the SIT2-FLCs' ones since the robustness measure β depends on the K_{min} and K_{max} values.

1) Increasing the rule size of the ST1-FLC structure

Firstly, it is worth to remind that it is not possible to generate the S-CC_{IT2}^{3R}, A-CC_{IT2}^{3R} and ISS-CC_{IT2}^{3R} when the ST1-FLC constructed from 50% overlapping Triangular antecedent MFs and Crisp consequent MFs (ST1-FLC-TC) and is composed of 3 or 5 rules as shown in section IV. Thus, it will be explored whether increasing the T1 fuzzy rule size to 9 or 15 will enable to duplicate the IT2-FM. Increasing the ST1-FLC rule size will give the opportunity to partition the input universe of discourse into more subintervals $[0,c_1]\cup[c_1,c_2]\ldots\cup[c_{n-1},1]$. Thus, more CA_{T1}s can be designed and naturally the input sensitivity of the T1-FM can be increased.

In the design of the ST1-FLC-TCs composed of 9 Rules (ST1-FLC-TC-9Rs), the Total Number of the Parameters (TNPs) to be designed is 8 since we will employ $c_p = -c_{-p}$ and $B_p = -B_{-p}$ to have a symmetrical T1-FMs (c_0=1, B_0=1). Thus, the ST1-FLC-TC-9R has 6 more design parameters than the SIT2-FLC. For the ST1-FLC-TC composed of 15 Rules (ST1-FLC-TC-15R), the TNPs to be tuned is 14, thus 12 more design parameters. The design of ST1-FLC-TCs can be accomplished according to CA_{T1}s presented in subsection III.A.2. Here, these parameter sets of the ST1-FLC-TCs will be optimized such that to minimize the *IAE* performance value via the genetic algorithm. The obtained optimal PSs of the ST1-FLC-TCs are given in Table IV, and their performance values and sector bounds are tabulated in Table III.

It can be seen that, in comparison with the ST1-FLC-TC-9R, the ST1-FLC-TC-15Rs resulted with lower *IAE* values and thus resulted with a better duplication of the IT2-FMs. However, as it can be seen from the variation of $\varepsilon[k]$ in Fig.7, even though the number of the rules of the ST1-FLC-TC has been increased, the T1-FMs were not able to exactly duplicate CC_{IT2}^{3R}s. For instance, from the variations of $\varepsilon[k]$ obtained for the duplication of A$-CC_{IT2}^{3R}$ (shown in Fig. 7b), it can be observed that the value of $\varepsilon[k]$ is relatively high especially when the input is close to "0". Thus, the performances of the ST1-FLCs will not be identical to the IT2 one, especially around the steady state. Also, the sector bound values of the T1-FM are not identical to the IT2 ones. Thus, the robustness measures β of the FMs will be different. (*A detailed robustness analysis is presented in next subsection*).

Note that, increasing even more the number of rules of the ST1-FLC-TCs will obviously result with a better matching performance but will also increase the TNPs and thus the design complexity. On the other hand, the CC_{IT2}^{3R}s were just generated by only tuning two parameters which clearly shows the design simplicity of the SIT2-FLCs. It can be concluded that the FOU gives the opportunity to generate CC_{IT2}^{3R}s which cannot be duplicated by 9 or 15 rule based ST1-FLC-TCs.

B. Employing different types of T1-FSs to the ST1-FLCs

Here, different types of the T1-FSs are employed to the antecedent and/or consequent part of the rules given in (27). Firstly, ST1-FLCs composed of 9 and 15 rules are designed where their antecedent part is defined with Triangular T1-FSs and their consequent part is defined with Linear functions (ST1-FLC-TLs) which are defined as $\varphi_i = p_i^0 + p_i^1\sigma$. For a ST1-FLC-TL composed of 9 Rules (ST1-FLC-TL-9R), there will be 9 antecedent MF parameters and 18 consequent MF parameters to be tuned; thus in total 27 design parameters. Similarly, for a ST1-FLC-TL composed of 15 Rules (ST1-FLC-TL-15R), the TNPs to be designed is 45. Secondly, Gaussian T1-FSs will be employed as the antecedent MFs of ST1-FLCs since they are powerful tools in representing nonlinearities. We will construct ST1-FLCs with Gaussian antecedent MFs and Crisp consequent MFs (ST1-FLC-GCs)

TABLE III. THE PERFORMANCE VALUES AND TNPS OF THE ST1-FLCS IN COMPARISON TO THEIR IT2 COUNTERPART

	TNPs	**S-CC_{IT2}^{3R}**		**A-CC_{IT2}^{3R}**		**ISS-CC_{IT2}^{3R}**	
		IAE	$[K_{min},K_{max}]$	*IAE*	$[K_{min},K_{max}]$	*IAE*	$[K_{min},K_{max}]$
SIT2-FLC	2	–	[0.6043,1.0000]	–	[1.0000,5.4054]	–	[0.8727,2.5901]
ST1-FLC-TC-9R	8	13.63	[0.6123,0.9000]	30.01	[0.9999,3.8300]	22.94	[0.8584,1.5800]
ST1-FLC-TC-15R	14	3.92	[0.6145,0.9423]	9.97	[1.0000,3.0200]	5.47	[0.8748,1.9030]
ST1-FLC-TL-9R	27	4.31	[0.6014,0.9015]	7.16	[0.9999,3.5300]	3.48	[0.8702,2.1680]
ST1-FLC-TL-15R	45	0.89	[0.6042,0.9508]	1.66	[1.0000,4.3300]	0.81	[0.8730,2.3800]
ST1-FLC-GC-9R	27	6.95	[0.5558,0.9512]	12.95	[0.9859,3.5600]	6.41	[0.8685,2.1344]
ST1-FLC-GC-15R	45	5.10	[0.5121,0.9723]	7.78	[0.9937,4.2790]	2.48	[0.8711,2.4442]
ST1-FLC-GL-9R	36	1.22	[0.6019,1.0100]	2.55	[1.0000,4.2800]	0.72	[0.8729,2.3092]
ST1-FLC-GL-15R	60	0.37	[0.6037,1.0000]	0.64	[1.0000,4.7150]	0.18	[0.8731,2.4449]

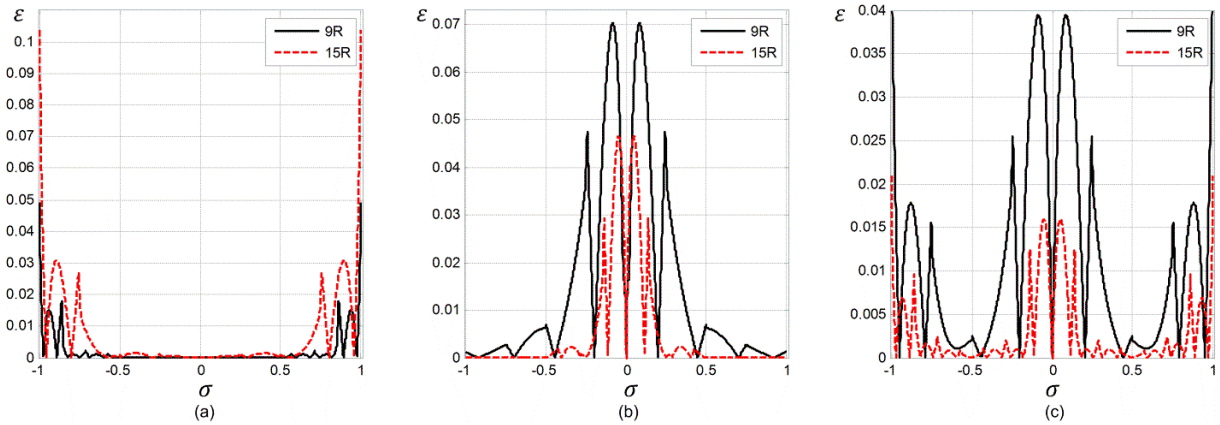

Fig.7. Illustration of the ε variations of the ST1-FLC-TCs for matching the (a) S-CC_{IT2}^{3R} (b) A-CC_{IT2}^{3R} (c) ISS-CC_{IT2}^{3R}

TABLE IV. THE OPTIMAL PARAMETERS OF THE ST1-FLC-TCS FOR MATCHING THE S-CC_{IT2}^{3R}, A-CC_{IT2}^{3R} AND ISS-CC_{IT2}^{3R}

Rule Size	(c_0,B_0)	(c_1,B_1)	(c_2,B_2)	(c_3,B_3)	(c_4,B_4)	(c_5,B_5)	(c_6,B_6)	(c_7,B_7)
Optimal Parameters of the ST1-FLC-TC for matching S-CC_{IT2}^{3R}								
9R	(0,0)	(0.24,0.15)	(0.49,0.31)	(0.74,0.48)	(0.74,0.89)	(-,-)	(-,-)	(-,-)
15R	(0,0)	(0.14,0.08)	(0.29,0.17)	(0.43,0.36)	(0.57,0.46)	(0.71,0.15)	(0.87,0.61)	(1.00,0.95)
Optimal Parameters of the ST1-FLC-TC for matching A-CC_{IT2}^{3R}								
9R	(0,0)	(0.23,0.54)	(0.50,0.68)	(0.75,0.85)	(1.00,0.99)	(-,-)	(-,-)	(-,-)
15R	(0,0)	(0.13,0.40)	(0.28,0.53)	(0.42,0.64)	(0.57,0.74)	(0.71,0.83)	(0.85,0.01)	(1.00,1.00)
Optimal Parameters of the ST1-FLC-TC for matching ISS-CC_{IT2}^{3R}								
9R	(0,0)	(0.24,0.36)	(0.50,0.49)	(0.75,0.64)	(1.00,0.95)	(-,-)	(-,-)	(-,-)
15R	(0,0)	(0.14,0.25)	(0.29,0.37)	(0.43,0.46)	(0.57,0.54)	(0.72,0.63)	(0.86,0.75)	(1.00,0.97)

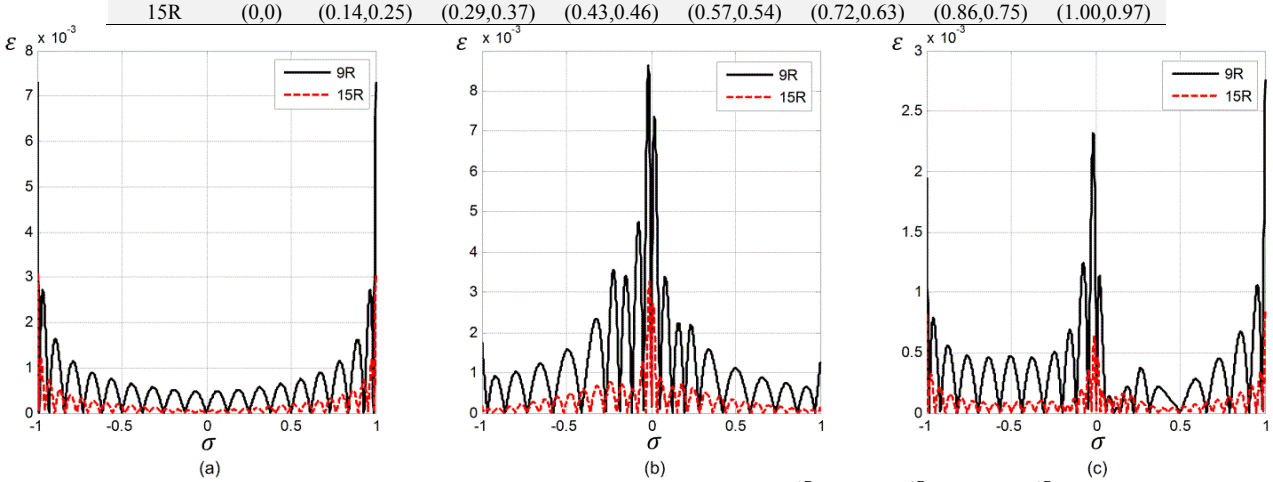

Fig.8. Illustration of the ε variations of the ST1-FLC-GLs (a) S−CC_{IT2}^{3R} (b) A−CC_{IT2}^{3R} (c) ISS−CC_{IT2}^{3R}

which are composed of 9 and 15 rules. Reminding that a Gaussian MF is defined with two parameters (its center and distribution), the TNPs to be designed for a ST1-FLC-GC of 9 Rules (ST1-FLC-GC-9R) is 27 while for a ST1-FLC-GC composed of 15 Rules (ST1-FLC-GC-15R) is 45. Furthermore, to provide even more degrees of freedom, ST1-FLCs are designed where their antecedent part is defined with Gaussian MFs while their consequent part is defined with Linear functions (ST1-FLC-GL). The TNPs for a ST1-FLC-GL of 9 Rules (ST1-FLC-GL-9R) is 36 and for a ST1-FLC-GL of 15 Rules (ST1-FLC-GL-15R) is 60.

Firstly, it is worth to underline that the CA_{T1}s presented in subsection III.A.2 could not be employed since they are only valid for ST1-FLC-TCs. In other words, the presented derivations and the analysis of the T1-FM cannot be used for the ST1-FLC-TL/GC/GLs since they are only valid for the ST1-FLC-TCs. Therefore, the design of these ST1-FLCs is accomplished via the ANFIS/Matlab toolbox (which applies a combination of the least-squares method and the backpropagation gradient descent method for training) by using the collected data set $[\sigma, \varphi_{o_{IT2}}]$. The performance measures and the sector bounds of the ST1-FLCs (ST1-FLC-TL/GC/GL) are given in Table III (since these ST1-FLCs will not be used in the rest of the paper, their PSs are not presented due to limited space). It can be seen that, it is possible to (almost) duplicate the IT2-FMs by increasing the rule size and employing different types of MFs. Here, the best matching performances have been obtained by the ST1-FLC-GL-15R which has 58 more design parameters than its IT2 counterpart. It can be seen from Fig.8 that the magnitude of $\varepsilon[k]$ values is relatively small for both the 9 and 15 rule based ST1-FLC-GLs. However, all these ST1-FLCs have been designed as black-box controllers to generate the IT2-FMs. Thus, the robust stability analysis and design methods cannot be employed since it has to be proven that Theorems 1-3 holds for these T1-FMs (the sector bound values given in Table I are calculated from the input/output data generated by the ST1-FLCs). From Fig.9, it can be also seen that the MFs of the ST1-FLC-TC/GL (for the duplication of the ISS−CC_{IT2}^{3R}) are not symmetrical with respect to the origin and are not %50

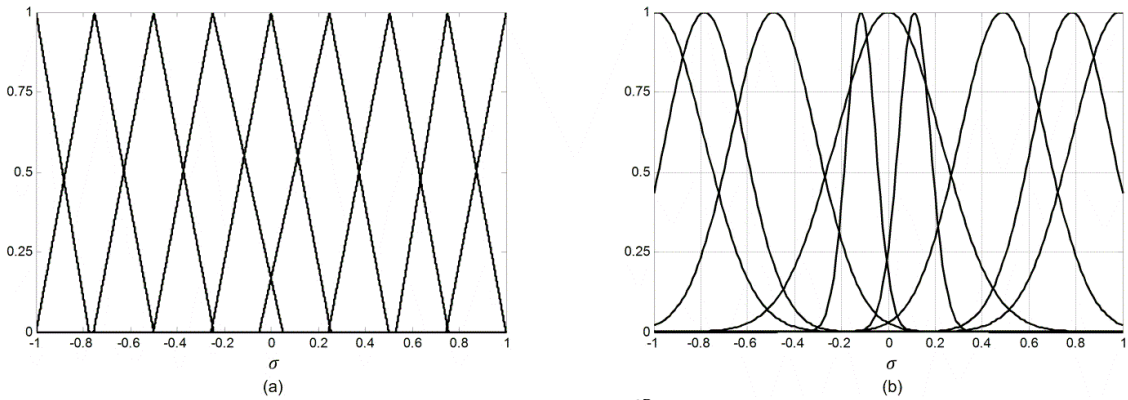

Fig.9. Illustration of the MFs for the generation of the ISS−CC_{IT2}^{3R} (a) ST1-FLC-TL-9R and (b) ST1-FLC-GL-9R

overlapping which results with a non-symmetric T1-FM. This can be also seen from Fig. 8 where the variations of ε is not symmetric with respect to the origin (Note that the error variations of the ST1-FLC-TCs are symmetrical in Fig.7). Thus, these T1 fuzzy systems cannot be transformed to Lure systems and their robust stability cannot be guaranteed. To sum up, although employing various MFs to the ST1-FLCs might enable to generate the IT2-FMs, the robustness analysis and design methods cannot be employed since the ST1-FLC-TL/GC/GL do not satisfy the properties of the ST1-FLC-TC.

C. Robust control performance comparison of the SLCs

In this subsection, the robustness of the SFLCs are examined and compared. We will first examine the robustness of two SIT2-FLCs which generate S$-$CC$^{3R}_{IT2}$ and A$-$CC$^{3R}_{IT2}$ to clearly show the role of the FOU on the robustness of the system. Therefore, we will present and examine their corresponding regions of stability (Ω) and robustness measures (β). Then, it will be examined whether their T1 counterparts will provide the same robustness measures. The robust stability analyses will be performed on a mass-damper-spring system which is shown in Fig.10a. The mass and damper constants are set as m=c=1 while the spring characteristic is defined as $t(x_1) = 3 - x_1^3$ [44]. The dynamic equations of the system are:

$$\begin{bmatrix}\dot{x}_{s1}\\ \dot{x}_{s2}\end{bmatrix} = \underbrace{\begin{bmatrix}0 & 1\\ -3 & -1\end{bmatrix}}_{A_{s0}}\begin{bmatrix}x_{s1}\\ x_{s2}\end{bmatrix} + \underbrace{\begin{bmatrix}0\\ 1\end{bmatrix}}_{b_{s0}}u + \underbrace{\begin{bmatrix}0\\ x_{s1}^3\end{bmatrix}}_{g(x_s)}$$
$$y = \underbrace{[1 \quad 0]}_{c_{s0}}\begin{bmatrix}x_{s1}\\ x_{s2}\end{bmatrix} \tag{66}$$

Here, x_{s1} and x_{s2} are the position and the velocity of the system, respectively.

To make a fair comparison, the baseline PID gains and SFs are set and fixed as K_P=0.1, K_D=2, K_I=0 and K_e=K_u=1, respectively for all the SFLCs in this study. To employ the stability analysis, we will transform the SFLC system into the system shown in Fig.1c. Therefore, by defining $x_1 = y$ and $x_2 = \dot{y} - K_D\varphi_o$, the following state space model is defined:

$$\begin{bmatrix}\dot{x}_1\\ \dot{x}_2\end{bmatrix} = \underbrace{\begin{bmatrix}0 & 1\\ -3 & -1\end{bmatrix}}_{A_1}\begin{bmatrix}x_1\\ x_2\end{bmatrix} + \underbrace{\begin{bmatrix}K_D\\ K_P - K_D\end{bmatrix}}_{b_1}\varphi_o + g(x)$$
$$\sigma = \underbrace{[-1 \quad 0]}_{c_1}\begin{bmatrix}x_1\\ x_2\end{bmatrix} \tag{67}$$

The corresponding normalized upper sector bound values are calculated as $\bar{K}_{S-IT2} = 0.3957$ $\left(K_{min_{IT2}} = 0.6043, K_{max_{IT2}} = 1\right)$ and $\bar{K}_{A-IT2} = 0.3778$ $\left(K_{min_{IT2}} = 1, K_{max_{IT2}} = 5.4054\right)$ for the S$-$CC$^{3R}_{IT2}$ and the A$-$CC$^{3R}_{IT2}$, respectively. Then, the state space representations of the fuzzy systems are obtained via the (18) that result with the transfer functions:

$$G_{S-IT2}(s) = \frac{2s + 0.1}{s^2 + 2.209s + 3.06} \text{ for S-CC}^{3R}_{IT2} \tag{68}$$

$$G_{A-IT2}(s) = \frac{2s + 0.1}{s^2 + 3s + 3.1} \text{ for A-CC}^{3R}_{IT2} \tag{69}$$

The Popov plots of $G_{S-IT2}(jw)$ and $G_{A-IT2}(jw)$ are shown Fig.10b and Fig.10c, respectively. It can be found that (19) is satisfied for $G_{S-IT2}(jw)$ if $r \geq 0.144$ while for $G_{A-IT2}(jw)$ if $r \geq 0.44$. We will set $r = 0.44$ which satisfies both cases. Then, the v and γ values are found as:

$$v_{S-IT2} = [-0.23 \quad -0.22]^T;\ \gamma_{S-IT2} = 3.41\} \tag{70}$$

$$v_{A-IT2} = [-0.06 \quad -0.22]^T;\ \gamma_{A-IT2} = 1.11\} \tag{71}$$

Now, if we set εW for both SIT2-FLCs systems as:

$$\varepsilon W = \begin{bmatrix}0.06 & 0\\ 0 & 0.06\end{bmatrix} \tag{72}$$

and solve (25), the P matrices are found as:

$$P_{S-IT2} = \begin{bmatrix}0.038 & -0.007\\ -0.007 & 0.036\end{bmatrix}$$
$$P_{A-IT2} = \begin{bmatrix}0.035 & -0.034\\ -0.034 & 0.035\end{bmatrix} \tag{73}$$

Here, if we set $\delta = 0.1$, (22) becomes as follows:

$$M_{S-IT2} = \{x \in R^4 | \|g(x)\|_2 \leq 0.237\|x\|_2\} \text{ for S-CC}^{3R}_{IT2} \tag{74}$$
$$M_{A-IT2} = \{x \in R^4 | \|g(x)\|_2 \leq 0.027\|x\|_2\} \text{ for A-CC}^{3R}_{IT2} \tag{75}$$

where the robustness measures of the fuzzy systems are obtained as $\beta_{S-IT2} = 0.237$ and $\beta_{A-IT2} = 0.027$. Moreover, the regions of attractions (Ω) can be determined via the Lyapunov function $V(x)$ since the IT2-FMs have closed form structures. Thus, the θ values are founds as $\theta_{S-IT2} = 0.060$ and $\theta_{A-IT2} = 0.167$ with respect to (74) and (75) and their stability regions are shown in Fig.10d. It can be observed that the robust stability of both SIT2-FLC systems is guaranteed but in different robustness measures and stability regions. The S-CC$^{3R}_{IT2}$ is potentially more robust against uncertainties since it has a bigger β_{S-IT2} value and a wider region of robust stability in comparison to the A$-$CC$^{3R}_{IT2}$ ones. Thus, the role of the FOU on the robustness of the SIT2-FLCs has been exposed from mathematical point of view.

The robustness analysis is also performed for the ST1-FLC-TC-15Rs since they provided the best matching performance. Their normalized sector bound values are found as $\bar{K}_{S-T1} = 0.3378$ $\left(K_{min_{T1}} = 0.6145,\ K_{max_{T1}} = 0.9423\right)$ and $\bar{K}_{A-T1} = 2.02$ $\left(K_{min_{T1}} = 1, K_{max_{T1}} = 3.02\right)$, After transforming the system into the configuration shown in Fig.1c, the robustness measures are found as $\beta_{S-T1} = 0.227$ and $\beta_{A-T1} = 0.0582$ for the ST1-FLCs which duplicate the S-CC$^{3R}_{IT2}$ and A-CC$^{3R}_{IT2}$, respectively. It can be observed that, although the ST1-FLC-TC-15Rs have satisfactory matching performance, the robustness measures of the T1 and IT2 structures are not identical ($\beta_{S-IT2} \neq \beta_{S-T1},\ \beta_{A-IT2} \neq \beta_{A-T1},$) since $\bar{K}_{A-IT2} \neq \bar{K}_{A-T1}, \bar{K}_{S-IT2} \neq \bar{K}_{S-T1}$. Thus, it can be concluded that the ST1-FLCs cannot duplicate the exact IT2-FMs and cannot also provide the same degree of robustness to system although they have more design parameters.

The control performances of the SFLCs are also examined and compared. It has been reported in [28], [43] that a controller which has a smooth control surface around the steady state is potentially more robust against nonlinearities and uncertainties. In this context, the control performance of the SIT2-FLC, which generates S$-$CC$^{3R}_{IT2}$, is compared with its ST1-FLC-TC-15R counterpart. The performances of SFLCs are investigated by examining how the controllers cope with different Initial Conditions (ICs) $[x_{10}, x_{20}]$ and their robustness against the present system nonlinearity $g(x_s)$. The performances of the SFLCs are illustrated in Fig.11 for the ICs [0,-1] (IC-1), [-0.2,0.9] (IC-2), [-0.2,-0.9] (IC-3) and [0.1,0.5] (IC-4).

It can be clearly seen that, in comparison to its T1 counterpart, the performance of SIT2-FLC is better while it is relatively more robust against the nonlinearity $g(x_s)$ and has the ability to cope better with the ICs. For instance, if we

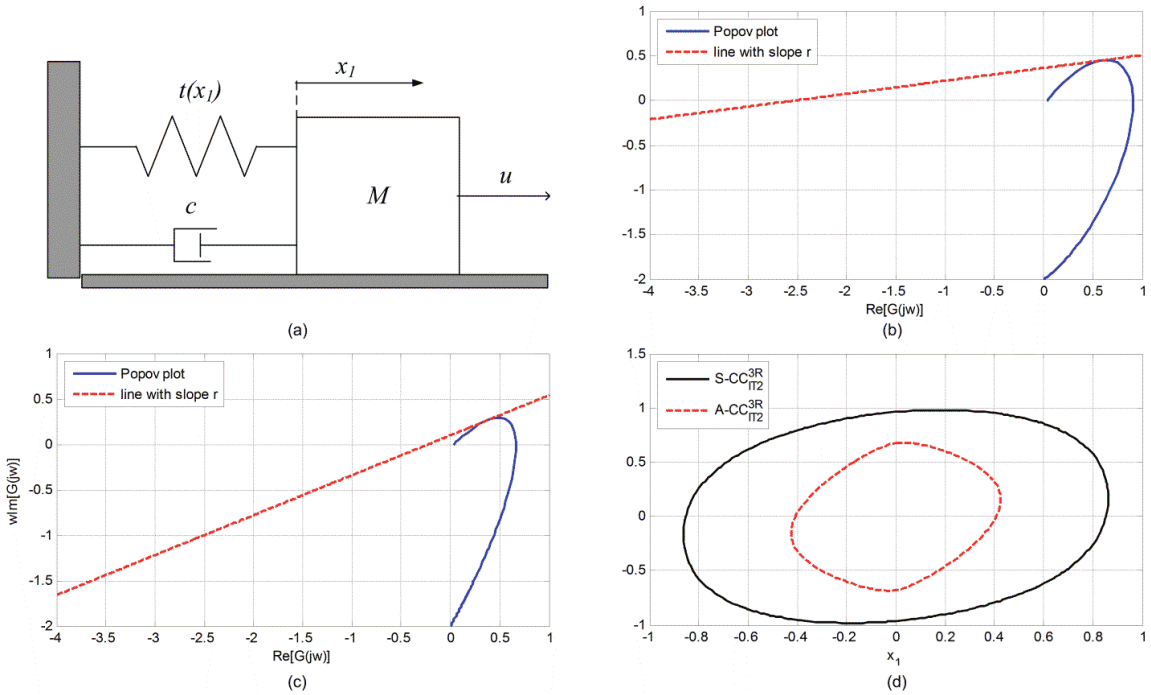

Fig.10. Illustration of the (a) mass-damper-spring system, (b) Popov plot of $G_{S-IT2}(jw)$ (c) Popov plot of $G_{A-IT2}(jw)$ (d) regions of stability of the SIT2-FLCs

examine the system responses for IC-1, when compared to the ST1-FLC, the SIT2-FLC systems has lower overshoot, undershoot values and provides a system response without oscillations. Similar comments can be also made for the system responses for the other ICs. The results also coincide with the calculated robustness measures of the SFLC, since the value β_{S-IT2} is relatively bigger than the value β_{S-T1}, the SIT2-FLC resulted with a relatively more robust performance in comparison to its T1 counterpart. It can be concluded that, although the ST1-FLC-TC-15R has more design parameters, the control performance of the SIT2-FLC is better than its T1 counterpart in presence of nonlinearity and for different ICs.

VI. Conclusions and Future Work

In this paper, the mathematical input–output relationship of the SIT2-FLC has been explicitly derived to present design methods and investigate the robustness of the SIT2-FLC with respect to the FOU parameters. In this context, it has been firstly proven that the IT2-FM is a symmetrical, continuous and sector bounded FM (which is also valid for its T1 counterpart). This gave the opportunity to link the robustness problem of the SIT2-FLC to a nonlinear controller and thus to guarantee its robustness with the aids of the Popov-Lyapunov method. Also, comparative explorations on the differences between the T1-FM and IT2-FM are provided with respect to their design parameters. Then, based on the observations, design strategies are presented for SIT2-FLCs composed of 3 and 5 rules without a need of an optimization procedure. It has been shown that the SIT2-FLC can generate commonly employed CCs by only tuning the size of the FOU. It has been also proven that the CC_{IT2}s cannot be generated by its T1 counterparts that are composed with identical number of rules.

Comprehensive simulation analyses are also presented to illustrate the presented analyses of the SFLC systems. At first, three SIT2-FLCs composed of 3 rules are designed such to generate commonly employed CCs by only tuning their FOU parameters (m_0, m_1) with respect to the derived CA_{IT2}s. This clearly shows the design simplicity of the SIT2-FLC. Then, since an IT2-FS embeds a huge number of T1-FSs, it has been investigated if these CC^{3R}_{IT2}s can be also generated by various ST1-FLCs (ST1-FLC-TC/TL/GC/GL). Based on the presented results, it has been concluded the ST1-FLC-TCs cannot generate the CC^{3R}_{IT2}s although they have more rules and more design parameters. On the other hand, the ST1-FLC-TL/GC/GLs were able to (almost) generate identical CC^{3R}_{IT2}s. However, since Theorem 1, 2 and 3 do not hold for these T1 fuzzy structures, the presented CC_{T1} design methods could not be employed and the robust stability of their T1 fuzzy systems can not be guaranteed. It has been concluded that that tuning the size of the FOU gives the opportunity to generate CC_{IT2}s which cannot be duplicated by various types of ST1-FLCs even though they have more design parameters (more degree of freedom) which shows the superiority of the SIT2-FLC in comparison with its T1 counterpart.

Moreover, comparative simulation results are presented to investigate the robustness of the SFLCs. Firstly, to show the role of the FOU parameters on the robustness of the SIT2-FLC, it has been shown that the stability of two SIT2-FLCs which have different sizes of FOUs is guaranteed but in different robustness measures. Thus, the direct relationship between the size of the FOU and robustness has been revealed from a mathematical point of view. Then, it has been exposed that the ST1-FLCs, which were constructed such that to duplicate the CC_{IT2}s, provide different robust control performances. Thus, by only tuning the size of the FOU with respect to the CA_{IT2}s, the SIT2-FLC can generate commonly employed CCs while also providing a certain degree of robustness that cannot be accomplished by its T1 counterpart.

The contributions of the study can be summarized as follows 1) investigating the robustness of SIT2-FLC in the framework of the well-developed nonlinear control theory, 2) providing theoretical explanations on the role of the FOU.

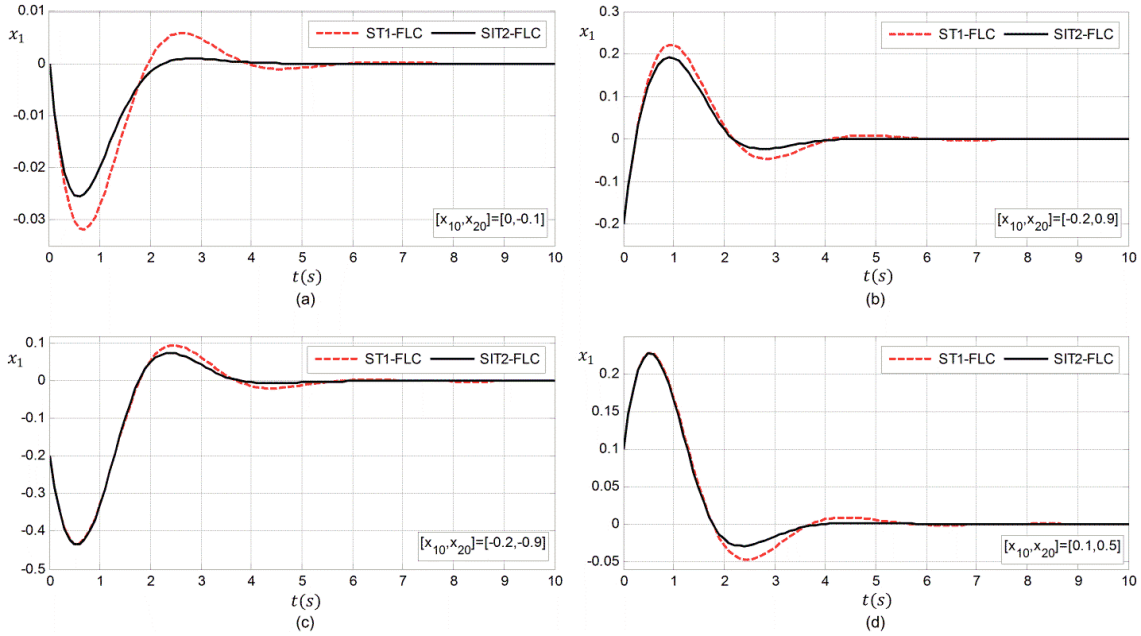

Fig.11. Illustration of the robust control performances of the SFLC systems for (a) IC-1 (b) IC-2 (c) IC-3 (d) IC-4

parameters on the performance and robustness of the SIT2-FLC, 3) presenting design methods to tune the FOU size of the SIT2-FLCs without a need of an optimization procedure. Future work will focus on extending the presented analyses to various types of IT2-FSs and IT2-FLC and relating transient state performance criteria (rise time, overshoot and settling time) with FOU parameters to open the door to a wider deployment of IT2-FLCs to real world control applications

APPENDIX A: PROOF OF THEOREM-2

(i) Let us firstly derive the T1-FM for $-\sigma \in [c_{-i-1}, c_{-i}]$ $(\varphi^{-i}_{o_{T_1}}(-\sigma))$ where $0 \notin [c_{-i-1}, c_{-i}]$. Reminding that $c_{-p} = -c_p$ and $B_{-p} = -B_p$, then $\varphi^{-i}_{o_{T_1}}(-\sigma)$ can be found as:

$$\varphi^{-i}_{o_{T_1}}(\sigma) = -\left(\sigma\, k^{i}_{T1} + \eta^{i}_{T1}\right) \tag{A.1}$$

Thus, it can be observed from (32) and (A.1) that $\varphi^{i}_{o_{T_1}}(\sigma) = -\varphi^{-i}_{o_{T_1}}(-\sigma)$ for $\forall \sigma \neq 0$. The T1-FMs for $\sigma \in [0, c_1]$ and $-\sigma \in [-c_1, 0]$ $\left(\varphi^{+0}_{o_{T_1}}(\sigma)\right.$ and $\left.\varphi^{-0}_{o_{T_1}}(-\sigma)\right)$ also satisfy the property since the T1-FMs will reduce to LMs. Thus, $\varphi_{o_{T_1}}(\sigma) = -\varphi_{o_{T_1}}(-\sigma)$ is always satisfied. It can be also seen from (34) that $\varphi_{o_{T_1}}(0) = 0$ is satisfied.

(ii) To prove the continuity of the FM, the points c_i, i.e., the cores of each MFs, must be examined. Thus, let us first examine the continuity around the point $c_0 = 0$ from (34):

$$\lim_{\sigma \to c_0^+} \varphi^{+0}_{o_{T_1}}(\sigma) = \lim_{\sigma \to c_0^-} \varphi^{-0}_{o_{T_1}}(\sigma) = 0 \tag{A.2}$$

Therefore, the T1-FM is continuous at the point $c_0 = 0$. Moreover, the continuity of $\varphi_{o_{T_1}}(\sigma)$ is examined for a generic input interval $[c_{i-1}, c_{i+1}]$ which is the union of the two subintervals $[c_{i-1}, c_i] \cup [c_i, c_{i+1}]$ (where $0 \notin [c_{i-1}, c_{i+1}]$). Thus, the critical point to be examined is c_i. In this context, the FM for $\sigma \in [c_{i-1}, c_i]$ $(\varphi^{i-1}_{o_{T_1}}(\sigma))$ is derived via (30) and is found as:

$$\varphi^{i-1}_{o_{T_1}}(\sigma) = \sigma\, k^{i-1}_{T1} + \eta^{i-1}_{T1} \tag{A.3}$$

where

$$k^{i-1}_{T1} = \frac{B_i - B_{i-1}}{c_i - c_{i-1}} \quad \eta^{i-1}_{T1} = \frac{B_{i-1}c_i - B_i c_{i-1}}{c_i - c_{i-1}} \tag{A.4}$$

Then, continuity of the FM around the critical point c_i can be examined as follows:

$$\lim_{\sigma \to c_i^+} \varphi^{i}_{o_{T_1}}(\sigma) = \lim_{\sigma \to c_i^-} \varphi^{i-1}_{o_{T_1}}(\sigma) = B_i \tag{A.5}$$

Thus, it can be concluded that the T1-FM is continuous in the interval $[c_{-n}, c_n]$. ■

APPENDIX B: PROOF OF THEOREM-3

We will first examine the FM for $\sigma \in [c_i, c_{i+1}]$ and then for $\sigma \in [0, c_1]$. For $\sigma \in [c_i, c_{i+1}]$, (36) can be reformulated as:

$$K^{i}_{min_{T_1}} \leq \Delta\varphi^{i}_{o_{T_1}} \leq K^{i}_{max_{T_1}} \tag{B.1}$$

where $\Delta\varphi^{i}_{o_{T_1}}(\sigma)$ is the gain variation of $\varphi^{i}_{o_{T_1}}(\sigma)$ is defined as:

$$\Delta\varphi^{i}_{o_{T_1}}(\sigma) = \frac{\varphi^{i}_{o_{T_1}}(\sigma)}{\sigma} = \frac{B_{i+1}(c_i - \sigma) + B_i(\sigma - c_{i+1})}{\sigma(c_i - c_{i+1})} \tag{B.2}$$

The candidate extrema points are the boundary points $\sigma_{c1} = c_i$, $\sigma_{c2} = c_{i+1}$ and the solutions of:

$$\frac{d\Delta\varphi^{i}_{o_{T_1}}(\sigma_{c3})}{d\sigma} = \frac{B_i c_{i+1} - B_{i+1}c_i}{\sigma^2(c_i - c_{i+1})} \tag{B.3}$$

Now, via the first order derivative test $\left(d\left(\Delta\varphi^{i}_{o_{T_1}}\right)/d\sigma > 0\right)$ under the constraints $B_i < B_{i+1}$ and $c_i < c_{i+1}$, it can be observed that $\Delta\varphi^{i}_{o_{T_1}}$ is always increasing function if $B_{i+1} > (B_i c_{i+1})/c_i$. Thus, the extrema values will be always on the boundary points (c_i, c_{i+1}) as follows:

$$K^{i}_{min_{T_1}} = B_{i+1}/c_{i+1} \quad K^{i}_{max_{T_1}} = B_i/c_i \tag{B.4}$$

If $B_i < B_{i+1} < (B_i c_{i+1})/c_i$, then the extrema values are:

$$K^{i}_{min_{T_1}} = B_i/c_i \quad K^{i}_{max_{T_1}} = B_{i+1}/c_{i+1} \tag{B.5}$$

For $\sigma \in [0, c_1]$, since the T1-FM is reduces to a LM, it is extrema values will be as follows:

$$K^{0}_{min_{T_1}} = 0 \quad K^{0}_{max_{T_1}} = B_1/c_1 \tag{B.6}$$

It can be concluded that $\varphi_{o_{T_1}}$ always belongs to a sector $\left[K_{min_{T_1}}, K_{max_{T_1}}\right]$ for $\sigma \in [c_{-n}, c_n]$. ■

APPENDIX C: PROOF OF THEOREM-4

(i) Let us firstly derive the IT2-FM for $-\sigma \in [c_{-i-1}, c_{-i}]$ $(\varphi^{-i}_{o_{IT2}}(-\sigma))$ where $0 \notin [c_{-i-1}, c_{-i}]$. From (49) and (50), $\varphi^{-i}_{o_{IT2}}(-\sigma)$ can be derived and is given in (C.1). By replacing the UMF and LMF values into (C.1), we can formulate:

$$\varphi^{-i}_{o_{IT2}}(-\sigma) = -(k^{i}_{IT2}(\sigma)\,\sigma + \eta^{i}_{IT2}(\sigma)) \tag{C.2}$$

Thus, it can be observed that $\varphi^{i}_{o_{IT2}}(\sigma) = -\varphi^{-i}_{o_{IT2}}(-\sigma)$ for $\forall\sigma \neq 0$ holds from (52) and (C.2). Now, to show that IT2-FM is also a symmetrical mapping for the interval $[-c_1, c_1]$ where $0 \in [-c_1, c_1]$, the FMs for $\sigma \in [0, c_1]$ and $-\sigma \in [-c_1, 0]$ will be examined. In this context, the FM for $-\sigma \in [-c_1, 0]$ $(\varphi^{-0}_{o_{IT2}}(-\sigma))$ is derived and found as:

$$\varphi^{-0}_{o_{IT2}}(-\sigma) = -k^{0}_{IT2}(\sigma)\,\sigma \tag{C.3}$$

From (55) and (C.3), it can be seen that $\varphi^{i}_{o_{IT2}}(\sigma) = -\varphi^{-i}_{o_{IT2}}(-\sigma)$ for $\forall\sigma \neq 0$ holds. Thus, the IT2-FM satisfies $\varphi_{o_{IT2}}(\sigma) = -\varphi_{o_{IT2}}(-\sigma)$ for $\sigma \in [c_{-n}, c_n]$ and $\varphi_{o_{IT2}}(0) = 0$.

(ii) To prove the continuity of IT2-FM, the cores of each antecedent IT2-FS (c_i) will be examined. It can be easily shown from (55) and (C.3) that

$$\lim_{\sigma\to c_0^{+}} \varphi^{+0}_{o_{IT2}}(\sigma) = \lim_{\sigma\to c_0^{-}} \varphi^{-0}_{o_{IT2}}(\sigma) = 0 \tag{C.4}$$

Thus, the IT2-FM is continuous at the point $c_0 = 0$. The continuity is also examined for a generic interval $[c_{i-1}, c_{i+1}]$ which is the union of the two subintervals i.e., $[c_{i-1}, c_i] \cup [c_i, c_{i+1}]$ where $0 \notin [c_{i-1}, c_{i+1}]$. Therefore we will examine the critical point c_i. In this context, the IT2-FM for $\sigma \in [c_{i-1}, c_i]$$(\varphi^{i-1}_{o_{IT2}}(\sigma))$ is derived via (51) and is found as:

$$\varphi^{i-1}_{o_{IT2}}(\sigma) = k^{i-1}_{IT2}(\sigma)\,\sigma + \eta^{i-1}_{IT2}(\sigma) \tag{C.5}$$

where

$$k^{i-1}_{IT2}(\sigma) = \frac{1}{2}\left(\frac{B_i - B_{i-1}m_{i-1}}{c_i m_{i-1} - c_{i-1} + \sigma(-m_{i-1}+1)} + \frac{B_{i-1} - B_i m_i}{c_{i-1}m_i - c_i + \sigma(-m_i+1)}\right) \tag{C.6}$$

$$\eta^{i-1}_{IT2}(\sigma) = \frac{1}{2}\left(\frac{B_i c_{i-1} - B_{i-1}c_i m_{i-1}}{-c_i m_{i-1} + c_{i-1} + \sigma(m_{i-1}-1)} + \frac{B_{i-1}c_i - B_i c_{i-1} m_i}{-c_{i-1}m_i + c_i + \sigma(m_i - 1)}\right) \tag{C.7}$$

Then, the continuity of the IT2-FM is examined as follows:

$$\lim_{\sigma\to c_i^{+}} \varphi^{i}_{o_{IT2}}(\sigma) = \lim_{\sigma\to c_i^{-}} \varphi^{i-1}_{o_{IT2}}(\sigma) = B_i \tag{C.8}$$

Thus, it can be concluded that the IT2-FM is always continuous in the interval $[c_{-n}, c_n]$. ■

APPENDIX D: PROOF OF THEOREM-5

We will first examine the IT2-FM for $\sigma \in [0, c_1]$ and then for $\sigma \in [c_i, c_{i+1}]$. In this context, (57) is firstly redefined as

$$K_{min_{IT2}} \leq \varphi_{o_{IT2}}(\sigma)\,/\sigma \leq K_{max_{IT2}} \tag{D.1}$$

Now, to derive the sector bounds of $\varphi_{o_{IT2}}(\sigma)$, let us define

$$\varepsilon_0(\sigma) \;= \varphi_{o_{IT2}}(\sigma) - \varphi_{o_{T1}}(\sigma) \tag{D.2}$$

where $\varepsilon_0(\sigma)$ is defined as the difference between the T1-FM and IT2-FM. It has been shown that T1-FM is bounded in Theorem 3, thus we only need to show that $\varepsilon_0(\sigma)$ is bounded to complete the proof. In this context, we will examine the gain variation of $\varepsilon_0(\sigma)$ which is defined as:

$$\Delta\varepsilon_0(\sigma) = \frac{\varepsilon_0(\sigma)}{\sigma} \tag{D.3}$$

(i) For $\sigma \in [0, c_1]$, (D.3) reduces to:

$$\Delta\varepsilon^0_o(\sigma) = P^0(\sigma)/Q^0(\sigma) = \frac{1}{2}B_1\left(\frac{(m_0m_1+1)c_1 - ((m_0-2)m_1+1)\sigma}{(m_0(c_1-\sigma)+\sigma)(c_1+(m_1-1)\sigma)} - \frac{2}{c_1}\right) \tag{D.4}$$

Now, let us examine the roots of $Q^0(\sigma)$ to investigate the existence of horizontal asymptotes:

$$\sigma_{Q_1^0} = c_1 m_0/(m_0-1) \quad \sigma_{Q_2^0} = -c_1/(m_1-1) \tag{D.5}$$

The derived roots will never lie in the interval $[0, c_1]$ since $c_1 > 0$ and $1 > m_i, m_{i+1} > 0$. Thus, $\varphi^0_{o_{IT2}}$ will always belong to a bounded sector $\left[K^0_{min_{IT2}}, K^0_{max_{IT2}}\right]$.

The parametric solutions of $K^0_{min_{IT2}}$ and $K^0_{max_{IT2}}$ can be obtained via by employing the first order derivative test to $\Delta\varepsilon^0_o(\sigma)$ under the constraint $0 < m_0, m_1 < 1$. Here, the candidate extrema points are $\sigma_{c1} = 0, \sigma_{c2} = c_1$ and σ_{c3} $\left(d\left(\Delta\varepsilon^0_o(\sigma)\right)/d\sigma = 0\right)$ that can be found via:

$$\sigma^2 + (a_1/a_2)\sigma + (a_0/a_2) = 0 \tag{D.6}$$

where

$$a_2 = (m_0-1)(m_1-1)(c_1((m_0-2)m_1+1)) \tag{D.7}$$

$$a_1 = c_1^2(m_i m_{i+1}+1)) \tag{D.8}$$

$$a_0 = (c_1^3(-(m_1-1)m_1m_0^2 + m_0 - 1)) \tag{D.9}$$

We will consider only the positive solution of (D.6), since $\sigma \in [0, c_1]$, which is derived as:

$$\sigma_{c3} = \frac{c_1 + c_1 m_0 m_1}{(m_0-2)m_1+1} - \sqrt{\frac{c_1^2 m_1 (m_0m_1-1)^2}{(m_0-1)(m_1-1)((m_0-2)m_1+1)^2}} \tag{D.10}$$

Now, to define $\mathbf{O_a}$ and $\mathbf{O_s}$, the roots of $P^0(\sigma)$ (the numerator of (D.4) are derived and are found as $\sigma_{P_1^0} = c_1$ and

$$\sigma_{P_2^0} = c_1(1 + m_0(m_1-2))/2(m_0-1)(m_1-1) \tag{D.11}$$

where $\sigma_{P_1^0}$ is the boundary point c_1. Here, $\sigma_{P_2^0}$ will provide information about the sign variation of $\Delta\varepsilon^0_o(\sigma)$. We can observe that $\sigma_{P_3^0}$ is in the interval $[0, c_1]$ under the conditions:

$$\left.\begin{array}{c} 0 < m_1 \leq 1/2 \;\&\; 0 < m_0 \leq m_{0_1} \\ \text{or} \\ 1/2 < m_1 \leq 1 \;\&\; m_{0_2} < m_0 \leq m_{0_1} \end{array}\right\} \Rightarrow \sigma_{P_3^0} \in [0, c_1] \tag{D.12}$$

where $m_{0_1} = 1/(2-m_1)$, $m_{o_2} = (2m_1-1)/m_1$. Now, by examining $d\left(\Delta\varepsilon^0_o(\sigma)\right)/d\sigma > 0$; we can conclude:

- If $0 < m_1 \leq 1/2$ and $0 < m_0 < m_{0_1}$, then $\Delta\varepsilon^0_o$ is an increasing function with respect to σ for the interval $0 < \sigma \leq \sigma_{c3}$ while a decreasing function for $\sigma_{c3} \leq \sigma \leq 1$. Thus, $K^0_{min_{IT2}} = k^0_{IT2}(\sigma_{c3})$ whereas $K^0_{max_{IT2}} = k^0_{IT2}(\sigma_{c1})$.
- If $0 < m_1 \leq 1/2$ and $m_{0_1} \leq m_0 < m_{0_3}$, then $\Delta\varepsilon^0_o$ is an increasing function with respect to σ if $0 < \sigma \leq \sigma_{c3}$ while a decreasing function if $\sigma_{c3} \leq \sigma \leq 1$ where m_{0_3} is:

$$\varphi^{-i}_{o_{IT2}}(-\sigma) = \frac{1}{2}\left(\frac{\overline{\mu}_{\tilde{A}_{-i-1}}(-\sigma)B_{-i-1} + \underline{\mu}_{\tilde{A}_{-i}}(-\sigma)B_{-i}}{\overline{\mu}_{\tilde{A}_{-i-1}}(-\sigma) + \underline{\mu}_{\tilde{A}_{-i}}(-\sigma)} + \frac{\underline{\mu}_{\tilde{A}_{-i-1}}(-\sigma)B_{-i-1} + \overline{\mu}_{\tilde{A}_{-i}}(-\sigma)B_{-i}}{\underline{\mu}_{\tilde{A}_{-i-1}}(-\sigma) + \overline{\mu}_{\tilde{A}_{-i}}(-\sigma)}\right) \tag{C.1}$$

$$m_{o_3} = \frac{1}{2}\left(\frac{1}{(m_1-1)m_1} + \sqrt{\frac{1-4(m_1-1)m_1}{(m_1-1)^2 m_1^2}}\right) \quad \text{(D.13)}$$

Thus, $K^0_{min_{IT2}} = k^0_{IT2}(\sigma_{c3})$ and $K^0_{max_{IT2}} = k^0_{IT2}(\sigma_{c2})$.

- If $0 < m_1 \le 1/2$ and $m_{0_3} \le m_0 \le 1$, then $\Delta\varepsilon^0_o$ is always a decreasing function with respect to σ for $\sigma \in [0, c_1]$. Therefore, $K^0_{min_{IT2}} = k^0_{IT2}(\sigma_{c1})$ and $K^0_{max_{IT2}} = k^0_{IT2}(\sigma_{c2})$.
- If $1/2 < m_1 \le 1$ and $0 < m_0 \le m_{0_2}$, then $\Delta\varepsilon^0_o$ is always an increasing function with respect to σ for $\sigma \in [0, c_1]$. Thus, $K^0_{max_{IT2}} = k^0_{IT2}(\sigma_{c1})$ and $K^0_{min_{IT2}} = k^0_{IT2}(\sigma_{c2})$.
- If $1/2 < m_1 \le 1$ and $m_{0_2} < m_0 \le m_{0_3}$, then $\Delta\varepsilon^0_o$ is an increasing function for $\sigma \in [0, \sigma_{c3}]$ while a decreasing function for $\sigma \in [\sigma_{c3}, 1]$. Thus, $K^0_{max_{IT2}} = k^0_{IT2}(\sigma_{c1})$ and $K^0_{min_{IT2}} = k^0_{IT2}(\sigma_{c3})$.
- If $1/2 < m_1 \le 1$ and $m_{0_3} < m_0 < 1$, then $\Delta\varepsilon^0_o$ is always a decreasing function with respect to σ for $\sigma \in [0, c_1]$. Thus, $K^0_{max_{IT2}} = k^0_{IT2}(\sigma_{c2})$ and $K^0_{min_{IT2}} = k^0_{IT2}(\sigma_{c1})$.

In Table A, the derived parametric solutions of $K^0_{min_{IT2}}$ and $K^0_{max_{IT2}}$ are summarized.

TABLE A. THE SECTOR BOUNDS OF THE IT2-FM FOR $\sigma \in [0, c_1]$

		$0 < m_1 \le 1/2$	
	$0 < m_0 < m_{0_1}$	$m_{0_1} \le m_0 < m_{0_3}$	$m_{0_2} \le m_0 \le 1$
$K^0_{min_{IT2}}$	$k^0_{IT2}(\sigma_{c3})$	$k^0_{IT2}(\sigma_{c3})$	$k^0_{IT2}(\sigma_{c1})$
$K^0_{max_{IT2}}$	$k^0_{IT2}(\sigma_{c1})$	$k^0_{IT2}(\sigma_{c2})$	$k^0_{IT2}(\sigma_{c2})$
		$1/2 < m_1 \le 1$	
	$0 < m_0 \le m_{0_2}$	$0 < m_0 \le m_{0_2}$	$0 < m_0 \le m_{0_2}$
$K^0_{min_{IT2}}$	$k^0_{IT2}(\sigma_{c2})$	$k^0_{IT2}(\sigma_{c2})$	$k^0_{IT2}(\sigma_{c2})$
$K^0_{max_{IT2}}$	$k^0_{IT2}(\sigma_{c1})$	$k^0_{IT2}(\sigma_{c1})$	$k^0_{IT2}(\sigma_{c1})$

(ii) For $\sigma \in [c_i, c_{i+1}]$, we can reformulate (D.3) as:

$$\Delta\varepsilon^i_o(\sigma) = \frac{P^i(\sigma)}{Q^i(\sigma)} \quad \text{(D.14)}$$
$$= \frac{\Delta B p_1 p_2 (2p_1 m_{i+1} - 2p_2 m_i + (p_1 + p_2)(m_i m_{i+1} + 1))}{2\Delta c \sigma (p_1 m_{i+1} - p_2)(-p_2 m_i - p_1)}$$

where $\Delta B = B_{i+1} - B_i, \Delta c = c_{i+1} - c_i \quad p_1 = \sigma - c_i$ and $p_2 = \sigma - c_{i+1}$. Here, by checking the roots of the denominator of $\Delta\varepsilon^i_o(\sigma)$ ($Q^i(\sigma) = 0$), we can observe if $\Delta\varepsilon^i_o(\sigma)$ is bounded or not, i.e. the existence of horizontal asymptotes. The roots of $Q^i(\sigma)$ are $\sigma_{Q^i_1} = 0$ and

$$\sigma_{Q^i_2} = \frac{(-c_i + c_{i+1} m_i)}{(-1 + m_i)} \quad \sigma_{Q^i_2} = \frac{(-c_{i+1} + c_i m_{i+1})}{(-1 + m_{i+1})} \quad \text{(D.15)}$$

The derived roots of $Q^i(\sigma)$ will never lie in the interval $[c_i, c_{i+1}]$ since $c_{i+1} > c_i$ and $1 > m_i, m_{i+1} > 0$. Thus, $\Delta\varepsilon^i_o(\sigma)$ does not have any horizontal asymptotes and therefore $\varphi^i_{o_{IT2}}$ is always sector bounded $\left[K^i_{min_{IT2}}, K^i_{max_{IT2}}\right]$.

The parametric solutions of $K^i_{min_{IT2}}$ and $K^i_{max_{IT2}}$ can be also derived by employing the first order derivative test to $\Delta\varepsilon^i_o(\sigma)$. The candidate points are $\sigma_{c1} = c_i, \sigma_{c2} = c_{i+1}$ and the roots of:

$$\frac{d\Delta\varepsilon^i_o(\sigma)}{d\sigma} = \frac{P^i(\sigma)\frac{dQ^i(\sigma)}{d\sigma} - Q^i(\sigma)\frac{dP^i(\sigma)}{d\sigma}}{Q^i(\sigma)^2} = 0 \quad \text{(D.16)}$$

(A.35) can be formulated as follows:

$$\sigma^4 + a_3/a_4\sigma^3 + a_2/a_4\sigma^2 + a_1/a_4\sigma + a_0/a_4 = 0 \quad \text{(D.17)}$$

where

$$a_4 = (m_i - 1)(m_{i+1} - 1)(c_i(m_i(m_{i+1} - 2) + 1) + c_{i+1}((m_i - 2)m_{i+1} + 1)) \quad \text{(D.18)}$$

$$a_3 = (m_i - 1)(m_{i+1} - 1)(c_i^2(m_i m_{i+1} + 1) + 2c_{i+1}c_i(-2m_i + (m_i - 2)m_{i+1} + 1) + c_{i+1}^2(m_i m_{i+1} + 1)) \quad \text{(D.19)}$$

$$a_2 = (c_i^3(-(m_i - 1)m_i m_{i+1}^2 + m_{i+1} - 1) - c_{i+1}c_i^2((m_i - 2)m_{i+1} + 1)(-7m_i + (5m_i - 6)m_{i+1} + 5) - c_i(m_i(m_{i+1} - 2) + 1)(-6m_i + (5m_i - 7)m_{i+1} + 5) + c_{i+1}^3(-(m_{i+1} - 1)m_{i+1}m_i^2 + m_i - 1)) \quad \text{(D.20)}$$

$$a_1 = 2c_i c_{i+1}(c_{i+1}(m_i(m_{i+1} - 2) + 1) + c_i((m_i - 2)m_{i+1} + 1))^2 \quad \text{(D.21)}$$

$$a_0 = c_i c_{i+1}(c_i - c_{i+1}m_i)(c_i m_{i+1} - c_{i+1})(c_{i+1}(m_i(m_{i+1} - 2) + 1) + c_i((m_i - 2)m_{i+1} + 1)) \quad \text{(D.22)}$$

Thus, there will be four more candidate extrema points $\sigma_{c3}, \sigma_{c4}, \sigma_{c5}$ and σ_{c6}. The explicit parametric solutions of (D.17) can be found via the algebraic root finding technique for quartic equations [46]. This will yield to the solution set:

$$\sigma_{c3,c4} = -a_3/4 + R/2 \pm D/2 \quad \text{(D.23)}$$
$$\sigma_{c5,c6} = -a_3/4 - R/2 \pm E/2 \quad \text{(D.24)}$$

where D and E are defined in (D.25) and (D.26), and R is as:

$$R = \sqrt{a_3^2/4 - a_2 + y_1} \quad \text{(D.27)}$$

Here, y_1 is the real root of the following cubic equation:

$$y^3 - a_2 y^2 + (a_1 a_3 - 4a_0)y + 4a_2 a_0 - a_1^2 - a_3^2 a_0 \quad \text{(D.28)}$$

However, the explicit derivation of the parametric solutions of the candidate extrema points is not straightforward. Though, since the design of the SIT2-FLC is accomplished based on the T1-FLC, the core values c_i, c_{i+1} in (D.17) are known. Thus, the explicit solution set can be derived via the first order derivative test with respect the FOU parameters via software like Mathematica/ Matlab.

In the light of (i), (ii), it can be concluded that the IT2-FM is always sector bounded. ■

$$D = \begin{cases} \sqrt{3a_3^2/4 - R^2 - 2a_2 + (4a_3a_2 - 8a_1 - a_3^3)/4R} & \text{for } R \neq 0 \\ \sqrt{3a_3^2/4 - 2a_2 + 2\sqrt{y_1 - 4a_0}} & \text{for } R = 0 \end{cases} \quad \text{(D.25)}$$

$$E = \begin{cases} \sqrt{3a_3^2/4 - R^2 - 2a_2 - (4a_3a_2 - 8a_1 - a_3^3)/4R} & \text{for } R \neq 0 \\ \sqrt{3a_3^2/4 - 2a_2 - 2\sqrt{y_1 - 4a_0}} & \text{for } R = 0 \end{cases} \quad \text{(D.26)}$$

REFERENCES

[1] R.-E. Precup and H. Hellendoorn, "A survey on industrial applications of fuzzy control," Comp. Ind., vol. 62, pp. 213–226, 2011.

[2] S. Galichet and L. Foulloy, "Fuzzy controllers: synthesis and equivalences," IEEE Trans. Fuzzy Syst.,vol. 3, no. 2, pp. 140–148, 1995.

[3] X. G. Duan, H. X. Li and H. Deng, "Effective tuning method for fuzzy PID with internal model control," Industrial & Engineering Chemistry Research, vol. 47, pp. 8317–8323, 2008.

[4] M. Mizumoto, "Realization of PID controls by fuzzy control methods," Fuzzy Sets and Systems, vol. 70, pp. 171–182, 1995.

[5] B. Mohan, A. Sinha, "The Simplest Fuzzy PID Controllers: Mathematical Models and Stability Analysis", Soft Computing, vol. 10, pp. 961–975, 2006.

[6] J. X. Xu, C. C. Hang and C. Liu, "Parallel structure and tuning of a fuzzy PID controller", Automatica, vol. 36, pp.673 -684 2000.

[7] H. Ying, "Theory and application of a novel fuzzy PID controller using a simplified Takagi-Sugeno rule scheme", Inf. Sci., vol. 123, no. 3-4, pp.281-293, 2000.

[8] Y. T. Juang, Y.T. Chang and C. P. Huang, "Design of fuzzy PID controllers using modified triangular membership functions", Information Sciences, vol. 178, Issue 5, Mar. 2008, pp. 1325-1333,

[9] R. K. Mudi and N. R. Pal, "A robust self-tuning scheme for PI- and PD-type fuzzy controllers," IEEE Trans. Fuzzy Syst., vol. 7, no.1, pp. 2–16, 1999.

[10] Z. W. Woo, H. Y. Chung and J. J. Lin, "A PID-type fuzzy controller with self-tuning scaling factors," Fuzzy Sets Systems, vol. 115, pp. 321–326, 2000.

[11] G. K. I. Mann, B. G. Hu, and R. G. Gosine, "Analysis of direct action fuzzy PID controller structures," IEEE Trans. Syst., Man, Cybern., B, Cybern., vol. 29, no. 3, pp. 371–388, 1999.

[12] B. Hu, G. K. I. Mann and R. G. Gasine, "New methodology for analytical and optimal design of fuzzy PID controllers," IEEE Trans. Fuzzy Syst., vol. 7, no.5, pp. 521–539, 1999.

[13] B. J. Choi, S. W. Kwak, and B. K. Kim, "Design and stability analysis of single-input fuzzy logic controller," IEEE Trans. Syst., Man, Cybern., vol. 30, no. 2, pp. 303–309, 2000.

[14] K. Ishaque, S.S. Abdullah, S.M. Ayob and Z. Salam, "Single Input Fuzzy Logic Controller for Unmanned Underwater Vehicle," Journal of Intelligent & Robotic Systems, vol.59, no.1, pp.87-100, 2010.

[15] F. Taeed, Z. Salam, and S. Ayob, "FPGA implementation of a single input fuzzy logic controller for boost converter with the absence of an external analog-to-digital converter," IEEE Trans. Ind. Electron., vol. 59, no. 2, pp. 1208–1217, Feb. 2012.

[16] P. S. Londhe, B. M. Patre, and A. P. Tiwari, "Design of single-input fuzzy logic controller for spatial control of advanced heavy water reactor," IEEE Trans. Nucl. Sci., vol. 61, no. 2, pp. 901–911, 2014.

[17] S. Yordanova, "Robust stability of single input fuzzy system for control of industrial plants with time delay," Journal of Intelligent and Fuzzy Systems, vol. 20, no. 1, pp. 29-43, 2009.

[18] T. Kumbasar and H. Hagras, "Big Bang-Big Crunch Optimization based Interval Type-2 Fuzzy PID Cascade Controller Design Strategy", Inf. Sci., vol. 282, pp. 277–295, 2014

[19] E. Yesil, "Interval type-2 fuzzy PID load frequency controller using Big Bang–Big Crunch optimization", Applied Soft Computing, vol. 15, pp. 100–112, 2014

[20] O. Castillo and P. Melin, "A review on the design and optimization of interval type-2 fuzzy controllers," Applied Soft Computing, vol. 12, pp. 1267–1278, 2012.

[21] S-K. Oh, H.-J. Jang, and W. Pedrycz, "A comparative experimental study of type-1/type-2 fuzzy cascade controller based on genetic algorithms and particle swarm optimization," Expert. Syst. Appl., vol. 38, no. 9, pp. 11217-11229, 2011.

[22] O. Castillo, R. Martínez, P. Melin, F. Valdez and J. Soria, "Comparative study of bio-inspired algorithms applied to the optimization of type-1 and type-2 fuzzy controllers for an autonomous mobile robot." Inf. Sci., vol. 19, no. 2 pp. 19-38, 2012.

[23] R. Martínez, O. Castillo, and L. T. Aguilar, "Optimization of interval type-2 fuzzy logic controllers for a perturbed autonomous wheeled mobile robot using genetic algorithms," Inf. Sci., vol. 179, no: 13, pp. 2158-2174, 2009.

[24] D. Wu and W. W. Tan, "Genetic learning and performance evaluation of type-2 fuzzy logic controllers," Int. J. Eng. Appl. Artif. Intell., vol. 19, no. 8, pp. 829–841, 2006.

[25] H. Hagras, "A Hierarchical Type-2 Fuzzy Logic Control Architecture for Autonomous Mobile Robots," IEEE Trans. Fuzzy Syst., vol. 12, no. 4, pp. 524-539, 2004.

[26] J. Mendel, Uncertain Rule-Based Fuzzy Logic Systems: Introduction and New Directions. Upper Saddle River, NJ: Prentice-Hall, 2001.

[27] Q. Liang and J.M. Mendel, "Interval type-2 fuzzy logic systems: theory and design," IEEE Trans. Fuzzy Syst., vol. 8, no.5, pp. 535-550, 2000.

[28] D. Wu, "On the Fundamental Differences between Type-1 and Interval Type-2 Fuzzy Logic Controllers," IEEE Trans. Fuzzy Syst., vol., 10, no.5, pp. 832- 848, 2012.

[29] D. Wu and J. M. Mendel, "On the continuity of type-1 and interval type-2 fuzzy logic systems," IEEE Trans. Fuzzy Syst., vol. 19, no. 1, pp. 179–192, 2011.

[30] H. Mo, F.Y. Wang, M. Zhou, R. Li and Z. Xiao, "Footprint of uncertainty for type-2 fuzzy sets," Inf. Sci., vol. 272, pp. 96-110, 2014.

[31] L. Chengdong, J. Yi, G. Zhang, "On the monotonicity of interval type-2 fuzzy logic systems" IEEE Trans. Fuzzy Syst., vol.12, no. 5, pp. 1197–1212, 2013.

[32] T. Kumbasar and H. Hagras, "A Self-Tuning zSlices based General Type-2 Fuzzy PI Controller," IEEE Trans. Fuzzy Syst., vol. 23, no. 4, pp. 991-1013, 2015.

[33] X. Du and H. Ying, "Derivation and analysis of the analytical structures of the interval type-2 fuzzy-PI and PD controllers." IEEE Trans. Fuzzy Syst., vol. 18, no. 4, pp. 802-814, 2010.

[34] M. Nie and W. W. Tan, "Analytical structure and characteristics of symmetric Karnik–Mendel type-reduced interval type-2 fuzzy PI and PD controllers," IEEE Trans. Fuzzy Syst., vol., 20, no.3, pp. 416-430, 2012.

[35] H. Zhou and H. Ying, " A Method for Deriving the Analytical Structure of a Broad Class of Typical Interval Type-2 Mamdani Fuzzy Controllers" IEEE Trans. Fuzzy Syst., vol. 21, no. 3, pp. 447-458, 2013.

[36] M. Biglarbegian, W. W. Melek, and J. M. Mendel, "On the stability of interval type-2 TSK fuzzy logic control systems," IEEE Trans. Syst., Man, Cybern. B, Cybern., vol. 40, no. 3, pp. 798–818, 2010.

[37] S. Jafarzadeh, S. Fadali, and A. Sonbol, "Stability analysis and control of discrete type-1 and type-2 TSK fuzzy systems: Part II control design", IEEE Trans. on Fuzzy Systems, vol. 19, no. 6, pp. 1001–1013, 2011.

[38] H. K. Lam and L. D. Seneviratne, "Stability analysis of interval type-2 fuzzy-model-based control systems", IEEE Trans. on Cybernetics, Part B, vol. 38, no. 3, pp. 617-628, 2008.

[39] T. Zhao and J. Xiao, "A new interval type-2 fuzzy controller for stabilization of interval type-2 T–S fuzzy systems", Journal of the Franklin Institute, vol. 352, no. 4, pp. 1627–1648, 2015.

[40] Q. Lu, P. Shi, H. K. Lam and Y. Zhao, "Interval Type-2 Fuzzy Model Predictive Control of Nonlinear Networked Control Systems", IEEE Trans. Fuzzy Syst., (Article in Press).

[41] H. Li, X. Sun, L. Wu, and H. K. Lam, "State and output feedback control of a class of fuzzy systems with mismatched membership functions," IEEE Trans. Fuzzy Syst., DOI: 10.1109/ TFUZZ. 2014. 2387876, 2014.

[42] H. Li, Y. Pan, and Q. Zhou, "Filter design for interval type-2 fuzzy systems with D stability constraints under a unified frame, IEEE Trans. Fuzzy Syst.," DOI 10.1109/TFUZZ.2014.2315658, 2014, 2014.

[43] T. Kumbasar, "A Simple Design Method for Interval Type-2 Fuzzy PID Controllers," Soft Computing, vol. 18, no. 7, pp. 1293-1304, 2014.

[44] C.-C. Fuh and P.-C. Tung, "Robust stability analysis of fuzzy control systems," Fuzzy Sets and Systems, vol. 88, pp. 289-298, 1997.

[45] K. H. Khalil, Nonlinear Systems, 2nd ed. Englewood Cliffs, NJ: Prentice-Hall, 1996.

[46] [Online]Available: http://mathworld.wolfram.com/QuarticEquation.html

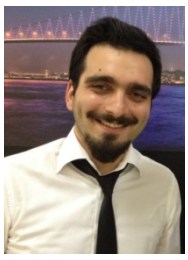

Tufan Kumbasar (M'13) received the B.Sc. and M.Sc. and Ph.D. degrees in Control and Automation Engineering from the Istanbul Technical University. He is currently an Assistant Professor in the Control and Automation Engineering Department, Faculty of Electrical and Electronics Engineering, Istanbul Technical University. His major research interests are in computational intelligence, notably type-2 fuzzy systems, fuzzy control, neural networks, evolutionary algorithms and control theory. He is also interested in process control, robotics, intelligent control and their real-world applications. He has currently authored more than 50 papers in international journals, conferences and books. Dr. Kumbasar received the Best Paper Award from the IEEE International Conference on Fuzzy Systems in 2015.